NATIONAL ADVISORY COMMITTEE FOR AERONAUTICS

TECHNICAL NOTE 2014

STATIC LONGITUDINAL STABILITY AND CONTROL OF A CONVERTIBLE-TYPE AIRPLANE AS AFFECTED BY ARTICULATED- AND RIGID-PROPELLER OPERATION

By Roy H. Lange and Huel C. McLemore

Langley Aeronautical Laboratory
Langley Air Force Base, Va.

Washington
February 1950

NATIONAL ADVISORY COMMITTEE FOR AERONAUTICS

TECHNICAL NOTE 2014

STATIC LONGITUDINAL STABILITY AND CONTROL OF A CONVERTIBLE-TYPE AIRPLANE AS AFFECTED BY ARTICULATED- AND RIGID-PROPELLER OPERATION

By Roy H. Lange and Huel C. McLemore

SUMMARY

The results of an investigation in the Langley full-scale tunnel of the static longitudinal stability and control of a convertible-type airplane (combination helicopter and airplane) as affected by articulated- and rigid-propeller operation are presented in this paper. The investigation included force measurements for a very large angle-of-attack range (from 12° to 90°) of the model with the all-movable horizontal tail installed and removed. The flight attitudes investigated include normal-flight conditions with full power applied and the convertible-flight region at high angles of attack including the transition to the hovering condition. The effects of ailavator and stability-flap deflection on control-surface effectiveness and on hinge moments were determined. The effects of propeller slipstream on the ailavator effectiveness at a static condition and at an angle of attack of 90° for low relative velocity conditions were also determined.

The results show that the destabilizing effect of propeller operation was more pronounced for rigid-propeller operation than for articulated-propeller operation because of the reduction in propeller normal force and the increment of positive pitching moment due to propeller articulation. The airplane for full-power operation has a positive-static-margin average of about 5 percent for articulated-propeller operation and about 3 percent for rigid-propeller operation over most of the lift-coefficient range from 0.50 (11.3° angle of attack) to about 1.90 (29.0° angle of attack). The all-movable horizontal tail is sufficiently powerful to trim the airplane throughout the lift-coefficient range (from 0.50 to 1.80) for full-power operation, although appreciably less deflection is required for trim with rigid-propeller operation. The destabilizing effect of full-power operation at moderate angles of attack was more pronounced for rigid-propeller operation. Full-power operation caused an increase in the ailavator effectiveness from -0.0050 per degree at a lift coefficient of 0.48 (11.3° angle of attack) to -0.0092 per degree at a lift coefficient of 1.84 (29.0° angle of attack) with articulated-propeller operation. The effectiveness,

however, was essentially constant at a value of about -0.0057 per degree throughout the lift-coefficient range with rigid-propeller operation. Full-power operation for articulated- and rigid-propeller operation increased the slope of the lift curve to about 0.068 and 0.070 per degree, respectively, as compared with the propeller-removed value of about 0.032 per degree. The airplane can be trimmed with ailavators alone in the high-angle-of-attack range up to 58° for rigid-propeller operation. No trim point is indicated, however, for any of the conditions for articulated-propeller operation. The results of the ailavator-effectiveness tests show that the ailavators have a high degree of effectiveness for the zero-velocity condition. For the condition at an angle of attack of 90° with a forward velocity of 22.5 miles per hour, the data indicate that very little, if any, of the propeller slipstream passes over the tail; however, the forward velocity is appreciably larger than would be expected for an actual flight condition. The stability flap can be used as a trimming device for the normal-flight attitudes; however, in the transition range the effectiveness is insufficient for trimming.

INTRODUCTION

Appreciable interest has been shown recently in the convertible-type airplane (combination helicopter and airplane) as a possible means of combining practical flight at very low speeds with efficient flight at moderately high speeds. For the very low speed region, numerous inherent aerodynamic problems are associated with stability and control for which very little information exists at the present time. Therefore, as a part of a general investigation in the Langley full-scale tunnel of a convertible-type airplane, tests have been conducted to determine the low-speed static longitudinal stability and control characteristics of a proposed military airplane designed for operation over a very wide angle-of-attack range. This airplane has an almost circular plan form with large-diameter articulated propellers located ahead of the wing tips. An all-movable horizontal tail (ailavators) is used to obtain both longitudinal and lateral control. A limited analysis of the power requirements of the subject airplane for low-speed conditions along with pertinent propeller-removed data as obtained from previous wind-tunnel tests is given in reference 1.

Propeller operation at high angles of attack was expected to contribute large unstable pitching-moment increments. One objective in the use of articulated propellers was to provide a decrease in the propeller normal force as compared with that for conventional propellers and thus improve the airplane longitudinal stability characteristics. Accordingly, it was planned, wherever possible, to provide comparisons of the effects of articulated-propeller and rigid-propeller (conventional) operation on the stability and control characteristics.

The results of the current investigation given herein include force measurements on the model obtained for a very large angle-of-attack range (from 12° to 90°) for conditions with the propellers removed and operating and with the all-movable horizontal tail installed and removed. The effects of ailavator and stability-flap deflection on control-surface effectiveness and hinge moments were also determined. The effects of propeller articulation on the static longitudinal stability and control were determined from tests with articulated- and rigid-propeller operation. Tests were also made of the model to determine the effects of propeller slipstream on the ailavator effectiveness for the static condition and also at an angle of attack of 90° for low relative velocity conditions.

COEFFICIENTS AND SYMBOLS

The results of the tests are presented as standard NACA coefficients of forces and moments. The data are referred to a system of axes coinciding with the wind axes. The pitching-moment coefficients are given about a center-of-gravity position located at a point on the root chord projected into the plane of symmetry from 26.3 percent of the mean aerodynamic chord.

C_L	lift coefficient (Lift/qS)
C_m	pitching-moment coefficient ($M/qS\bar{c}$)
C_{D_R}	resultant drag coefficient (D_R/qS)
C_h	hinge-moment coefficient ($H/qb'c'^2$)
Q_c	torque coefficient ($Q/2qD^3$)
c_{l_d}	propeller-blade-section design lift coefficient
q	free-stream dynamic pressure $\left(\frac{1}{2}\rho V^2\right)$
V	velocity
S	wing area; 47.444 square feet on model
ρ	mass density of air
α	angle of attack of thrust axis relative to free-stream direction, degrees
α_u	uncorrected angle of attack

$\bar{c}$	mean aerodynamic chord; 6.61 feet on model
D_R	resultant drag with propellers operating
M	pitching moment
ϵ_{eff}	effective downwash angle, degrees
V/nD	propeller advance-diameter ratio
D	propeller diameter; 5.33 feet on model
Q	torque per propeller
β	propeller-blade angle measured at 0.70 radius, degrees
θ	propeller-blade angle measured at any radius, degrees
r	radius at any propeller-blade section
R	propeller-tip radius
x	fraction of propeller-tip radius (r/R)
b	propeller-blade chord
h	propeller-blade-section maximum thickness
H	hinge moment of control surface
c'	root-mean-square chord of control surface behind hinge line
b'	control-surface span along hinge line
δ	control-surface deflection, degrees
C_{m_δ}	rate of change of pitching-moment coefficient per degree of control-surface deflection
C_{h_δ}	rate of change of hinge-moment coefficient per degree of control-surface deflection

Subscripts:

a	ailavator
f	stability flap

p propeller

t all-movable horizontal tail

MODEL

The configuration tested was the $\frac{1}{3}$-scale model of a convertible-type airplane. The description of the model and the tunnel-support arrangement are given in reference 1. A three-view drawing of the model and its geometric characteristics are given in figure 1. Photographs of the model mounted in the Langley full-scale tunnel are given as figure 2.

The model was powered by a 200-horsepower, water-cooled, electric induction motor. This motor was submerged spanwise in the model, and power was transmitted from the motor to the propellers by means of extension shafts through right-angle gear drives at the wing tips. The propeller installation at each wing tip consisted of 2 two-blade propellers mounted in tandem so as to form a four-blade configuration. These tandem propellers rotated in the same direction, but the propellers at each wing tip rotated upward at the wing center section.

The propeller blades were free to flap forward and rearward 10° from the perpendicular to the propeller axis as they rotated. The blades of each propeller were so interconnected that as one blade flapped forward the opposite blade flapped rearward. In addition, as a blade flapped forward the propeller-hub mechanism caused the blade pitch angle to decrease, and conversely, as the blade flapped rearward the pitch angle was increased. This load-relieving mechanism was believed necessary by the airplane designer as the result of an analysis which included considerations of propeller stability, blade loads, and uniformity of disc-thrust loading. The propeller-blade plan-form curves are given in figure 3. For the rigid-propeller tests the blades were locked so that no blade flapping occurred.

The propeller torque was determined from the calibration of motor torque as a function of minimum input current to the motor.

Stability flaps are provided (see fig. 1) for the purpose of trimming out most of the destabilizing pitching moment due to propeller operation.

The movable control surfaces on the model were hydraulically actuated by remote control. Electrical position indicators and strain gages were used to measure the control-surface deflections and hinge moments, respectively. The strain gages were located only on the right control surfaces.

METHODS AND TESTS

Force tests were made of the model for a range of angles of attack from 12° to 90° and for tunnel velocities from about 23 to 55 miles per hour.

Inasmuch as the effects of propeller operation on the lift of the subject airplane are large, especially at the higher angles of attack, the determination of the propeller-operating conditions for simulated full-power operation required the duplication of the correct blade angle and advance ratio in addition to the torque coefficient. The methods used to obtain these propeller-operating conditions are described in reference 1. The three attitudes investigated are shown in figure 4, both for articulated- and rigid-propeller operation. The propeller-blade-angle settings of figure 4 are 1° less than those given in reference 1 because of a correction found necessary in the blade-angle measuring device.

Tests were made with articulated and rigid propellers at each of the propeller-operating conditions with the all-movable horizontal tail installed and removed. For the tests with the all-movable horizontal tail removed the angle of attack, propeller-blade angle, and propeller advance-diameter ratio used were the same as those used with the tail installed so that a close simulation of the full-power operating conditions resulted.

The ailavator and stability-flap-effectiveness tests were made at angles of attack of 11.3°, 23.1°, and 29.0° for simulated full-power operation. Similar tests were made at high angles of attack for conditions of steady, unaccelerated flight $(C_{D_R} = 0)$ as determined from reference 1 and from thrust calibrations. The ailavator-effectiveness tests were made for articulated- and rigid-propeller operation; whereas the stability-flap-effectiveness tests were made only for articulated-propeller operation. For the ailavator-effectiveness tests, the ailavators were deflected through a range from -48° to 4° with $\delta_f = 0°$. For the stability-flap-effectiveness tests, the stability flaps were deflected through a range from -16° to 30°. For the stability-flap effectiveness tests at angles of attack of 11.3°, 23.1°, and 29.0°, the ailavators were set for trim. At the higher angles of attack, the ailavators were set at the maximum deflection of -48°, inasmuch as the ailavator tests indicated that the model could not be trimmed at these attitudes. Hinge moments of only the right control surfaces were recorded.

Tests were made at an angle of attack of 90° to determine the effects of propeller operation on the ailavator-control effectiveness for low-forward-velocity conditions. For the low-speed condition, the tests were

made at a tunnel velocity of approximately 22.5 miles per hour with propellers removed and for propeller operation at maximum thrust as limited by a maximum allowable propeller speed of 2500 rpm. The static test was made with the propellers operating at 2500 rpm. For these tests, the ailavators were deflected through a range from -48° to 8° with $\delta_f = 0°$. Hinge moments of only the right ailavator were recorded.

Tests were attempted in order to determine, if possible, the stability and control characteristics of the model in attitudes representing vertical descent; however, the tests were terminated before any data were recorded due to excessive vibration of the model in the air stream.

RESULTS AND DISCUSSION

The presentation of the test results and the analysis of the data have been grouped into two main sections. The first section deals with the static longitudinal stability and control characteristics of the airplane for normal-flight attitudes with full power applied. These results are given in the summary curves of figures 5 to 14 which are derived from the original test data presented in figures 15 to 18. The second section presents results for the static longitudinal stability and the control-surface-effectiveness tests for the airplane in the convertible-flight region at high angles of attack including the transition to the hovering condition (figs. 19 to 22). Wherever possible the comparisons of the effects of articulated- and rigid-propeller operation on the stability and control characteristics are included.

The data have been corrected for stream alinement, blocking, and jet-boundary effects. No tare corrections were applied to the data for the effects of the support strut; however, it is felt that these effects would produce no significant change in the stability characteristics.

Static Longitudinal Stability and Control at Normal-Flight Attitudes

Longitudinal stability.- The static longitudinal stability of the airplane is described by the stick-fixed neutral-point curves of figure 6 which were determined from the curves of figure 5 by method 1 of reference 2. In general, for the normal center-of-gravity location at 26.3 percent of the mean aerodynamic chord, a positive-static-margin average of about 5 percent for articulated-propeller operation and about 3 percent for rigid-propeller operation results over most of the lift-coefficient range from 0.50 to 1.90. At the highest lift coefficient measured ($C_L \approx 1.9$), however, no appreciable difference in the stick-fixed stability between the two modes of propeller operation is

present. As explained in more detail subsequently, the greater stability of the airplane for articulated-propeller operation can be attributed to the reduction in the destabilizing propeller normal force for this mode of propeller operation.

An indication of the stick-free stability of the airplane given by the variation of the pitching-moment coefficient for $C_{h_a} = 0$ with lift coefficient is presented in figure 7 for the tab-neutral condition. For articulated-propeller operation a large amount of stability is indicated for a lift-coefficient range from 0.46 to 0.56 after which neutral stability is indicated. With rigid-propeller operation, a large amount of stability is indicated for only a very small, low-lift-coefficient range after which the stick-free stability decreases with increasing lift coefficient.

Longitudinal control.- The magnitude of the ailavator deflections required for trim shown in figure 8 indicate that the all-movable horizontal tail is sufficiently powerful to trim the airplane throughout the lift-coefficient range from 0.50 to 1.80 for both the articulated- and the rigid-propeller operation. The variations shown are stable but a more desirable variation is given with rigid-propeller operation. Appreciably less ailavator deflection is required for trim, however, for rigid-propeller operation as compared with articulated-propeller operation with the difference in the high-lift-coefficient range amounting to about 14° which is about one-half the deflection required with articulated-propeller operation.

A reversal in $\left(C_{h_\delta}\right)_a$ $\left(\text{measured at } C_{h_a} = 0 \text{ to compare with the propellers-removed data of reference 1}\right)$ from positive to negative values is shown in figure 9 up to a lift coefficient of 0.60 for articulated- and rigid-propeller operation. At higher lift coefficients $\left(C_{h_\delta}\right)_a$ decreases negatively with increasing lift coefficient throughout the range investigated. The reversal in $\left(C_{h_\delta}\right)_a$ at the lower lift coefficients indicates that there is an overbalance of the surface at the low deflections. This reversal was also noted for the model with propellers removed (see reference 1), and a comparison shows that propeller operation intensified the reversal.

Contribution of the tail to stability.- For convenience in the interpretation of the stability characteristics of the airplane, the increments in pitching-moment coefficient and lift coefficient due to propeller operation for the model with the all-movable horizontal tail removed are shown in figure 10. These results were obtained from figure 18. Rigid-propeller operation contributes appreciably more destabilizing effect than that shown for articulated-propeller operation as a result of the decreased normal force on the articulated propellers, as noted previously.

The change in pitching-moment coefficient and lift coefficient due to propeller operation for a conventional airplane with the tail removed may be determined from considerations of the direct effect of the propeller forces and of the slipstream effect on the wing as described in reference 3; accordingly by using the methods of reference 3, calculations of ΔC_{m_p} and ΔC_{L_p} were made and are presented in figure 10 for comparison with the experimental values. Such a comparison can be made only for rigid-propeller operating conditions inasmuch as no methods are available for predicting the force and slipstream characteristics of an articulated propeller. The poor agreement shown in figure 10 may be attributed largely to the effects on the induced flow of the unusual propeller installation at the wing tips of the very low aspect ratio wing.

By a comparison of the results of the tests of the model with the all-movable horizontal tail installed with the propellers removed and with the propellers operating (see fig. 17), the increments of pitching-moment coefficient of the wing and tail due only to the effects of propeller operation have been determined and are shown in figure 11. The increments of tail pitching-moment coefficient due to propeller operation are small, especially for articulated-propeller operation.

The total contribution of the all-movable horizontal tail to the longitudinal stability of the airplane is shown in figure 12 for the propeller-removed and the propeller-operating conditions. In general, both the articulated- and the rigid-propeller operation caused an increment of negative pitching-moment coefficient to be produced by the tail. At the higher angles of attack, the increment in negative pitching-moment coefficient decreases for the articulated-propeller operation such that at an angle of attack of 29° the value is the same as that for the model with the propellers removed. The normal force on the all-movable horizontal tail is positive throughout the angle-of-attack range for the propeller-removed as well as for the propeller-operating conditions.

By a comparison of the pitching-moment coefficients of the model with the all-movable horizontal tail installed and removed, the effective downwash angles at the tail were computed and plotted in figure 13 against angle of attack. The effective downwash angle is defined by the tail incidence for which the contribution of the tail to the total pitching moment is zero. As shown in figure 13, the effective downwash at the tail is small for both articulated- and rigid-propeller operation. A stable upwash at the tail is shown for articulated-propeller operation which remains essentially constant with angle of attack; whereas for rigid-propeller operation the small upwash at low angles of attack gradually changes to a downwash at the higher angles of attack.

Control-surface-effectiveness results.- The ailavator effectiveness $\left(C_{m_\delta}\right)_a$ was obtained from the results of figure 15 and is shown plotted against lift coefficient in figure 14. The ailavator effectiveness, for articulated-propeller operation, increased from -0.0050 per degree at $C_L = 0.48$ to -0.0092 per degree at $C_L = 1.84$. For rigid-propeller operation, however, the ailavator effectiveness was essentially constant at a value of about -0.0057 per degree throughout the lift-coefficient range. The data indicate, therefore, that the tail is more favorably located with respect to the propeller slipstream for articulated-propeller operation than for rigid-propeller operation. The ailavator effectiveness of the model with propellers removed but with engine-air ducts and canopy installed (see reference 1) was about -0.0050 per degree throughout the angle-of-attack range investigated. This value is offered for comparison with the propellers-operating data for in this instance the differences in model configuration are believed to have little effect on the control-surface effectiveness.

The results of the stability-flap tests are presented in figure 16 and show the variations with flap deflection of C_m, C_L, C_{h_f}, and C_{h_a}. For these tests the ailavators were set at the deflection required for trim at each angle of attack. The flap effectiveness $\left(\left(C_{m_\delta}\right)_f, \delta_f = 0^\circ\right)$ increases from a value of about -0.0025 per degree at an angle of attack of 11.3° to -0.0032 at an angle of attack of 23.1° and then decreases to -0.0020 at an angle of attack of 29.0°. The flap effectiveness $\left(C_{m_\delta}\right)_f$ with propellers removed for the same model configuration increases from -0.0020 per degree at an angle of attack of 11.3° to -0.0026 for angles of attack of 23.2° and 29.3° (reference 1). Propeller operation, therefore, has a small effect on the flap effectiveness. The stability flap, therefore, can be used as a trimming device for normal-flight attitudes.

The flap hinge-moment variation $\left(C_{h_\delta}\right)_f$ measured at zero flap deflection increases from about -0.0015 per degree at an angle of attack of 11.3° to -0.0049 at an angle of attack of 23.1° and then decreases to -0.0042 at an angle of attack of 29.0° for the model with propellers operating (fig. 16). The value of $\left(C_{h_\delta}\right)_f$ increases rapidly in a negative direction with increasing positive and negative flap deflections but shows a marked reduction in hinge moments with angle of attack for positive flap deflections greater than about 16°. Propeller operation also has a small effect on the rate of change of hinge-moment coefficient with flap deflection $\left(C_{h_\delta}\right)_f$ since the maximum propellers-removed value was -0.0032 per degree at an angle of attack of 29.3° (reference 1). As shown in figure 16, flap deflection has no appreciable effect on the ailavator hinge-moment coefficients for the conditions investigated.

The effect of flap deflection on the lift coefficient is small with the propellers operating, and this same effect was also noted in reference 1 with propellers removed. A maximum increase in lift coefficient of only 0.19 (at $\alpha = 29.0^{\circ}$) is measured for full positive flap deflection with propellers operating (fig. 16) as compared with a value of 0.12 at $\alpha = 11.3^{\circ}$ with propellers removed (reference 1).

Effect of propeller operation on lift at normal-flight attitudes.- With propellers removed the model has a low value of lift-curve slope (0.032 per degree at $C_L = 0.6$) which is characteristic of low-aspect-ratio wings. Full-power operation more than doubled the lift-curve slope with values of 0.068 and 0.070 per degree being measured at $C_L = 0.6$ for articulated- and for rigid-propeller operation, respectively. (See fig. 17.) The rapid increase in lift due to propeller operation at the higher angles of attack was discussed in reference 1 where calculations showed that about one-third to one-half of the total increase in lift due to propeller operation results from the lift component of the propeller resultant force.

Longitudinal Stability and Control in the Transition Range

The airplane was designed for possible operation above the normal stall of the wing through the transition range to the hovering attitude. As pointed out previously, in this high-angle-of-attack region propeller operation was expected to be highly destabilizing and, therefore, the longitudinal stability and control was expected to be critical; also, propeller articulation was expected to make the problems of stability and control in the transition range less difficult.

Longitudinal stability.- As an indication of the longitudinal stability of the airplane in the transition range, curves showing the variations of C_m with C_L for constant ailavator settings are given in figure 19. The data for figure 19 were obtained from the curves of figure 20. The large lift coefficients for the model measured in the high-attitude transition range indicate that a greater part of the total lift is being assumed by the vertical component of the propeller thrust. The variations of C_m with C_L for full-power rigid-propeller operation near trim indicate that the airplane will be unstable in the transition range investigated. The instability of the airplane with rigid-propeller operation is due largely to the unstable pitching-moment contribution of this type of propeller operation. The effect of propeller articulation is to decrease markedly the unstable contribution of the propeller; however, the decrease is excessive with the result that the airplane cannot be trimmed for any of the conditions investigated. Because no trim points are shown for the airplane with articulated-propeller operation, the variations of C_m with C_L do not necessarily indicate

the longitudinal stability characteristics of the airplane, at least for the particular configuration investigated.

The airplane can be trimmed with ailavators alone in the high-angle-of-attack range up to about 58° for rigid-propeller operation. (See figs. 19 and 20.) The ailavator deflection required for trim increases from -26.8° at $\alpha \approx 41°$ to -32.8° at $\alpha \approx 46°$, then decreases to about 0° at $\alpha \approx 58°$. These results indicate that at angles of attack up to 46° the large negative pitching moments associated with the wing alone with propellers removed (reference 1) predominate over the positive pitching moments created by the propeller normal force. At an angle of attack of 58°, however, these effects counterbalance one another with the result that very little ailavator deflection is required for trim. An increase in the angle of attack to 69° results in a condition where the model cannot be trimmed with rigid propellers operating because of the predominate effect of the destabilizing propeller normal force.

Ailavator effectiveness.- The ailavator effectiveness $\left(C_{m_\delta}\right)_a$ at trim for rigid-propeller operation increases slightly from a value of about -0.0064 per degree at an angle of attack of 41° to -0.0074 per degree at an angle of attack of 46°, then decreases to -0.0040 per degree at an angle of attack of 58°. (See fig. 20.) Although no trim points are indicated for any of the other conditions investigated, the ailavator effectiveness for articulated-propeller operation is much lower than for rigid-propeller operation. The variation of C_{h_a} with δ_a is also larger for rigid-propeller operation than for articulated-propeller operation except at an angle of attack of 69°. It is interesting to note that for angles of attack of 41° and 46° the ailavator effectiveness for rigid-propeller operation is greater than that measured for the normal-flight attitudes.

In order to evaluate the longitudinal control characteristics of the airplane for the hovering attitude the ailavator effectiveness was determined with articulated-propeller operation only, both for the zero-forward-velocity condition and for as low a forward velocity as could be obtained in these tests which was about 23 miles per hour. The results are given in figure 21 for an angle of attack of 90°. For the static test with the ailavators immersed only in the propeller slipstream, the pitching moment increases rapidly with increasing ailavator deflection up to $\delta_a = -16°$ after which, due to ailavator stalling, the pitching moments remain essentially constant. (See fig. 21(a).) No trim point is indicated for the range of ailavator deflection investigated. The hinge moments increase slightly with ailavator deflection up to -16° after which a rapid increase occurs with increasing deflection. With a forward speed of 22.5 miles per hour and with articulated-propeller operation, the ailavator effectiveness is essentially zero throughout

the deflection range. The associated hinge moments for this condition at the high deflections are much lower than those measured for the zero-forward-velocity condition. The results indicate, therefore, that only a very small part, if any, of the propeller slipstream passes over the tail when the airplane possesses a forward speed of 22.5 miles per hour and that the airplane cannot be trimmed. It should be emphasized here, however, that for the model angle of attack investigated, the forward velocity of 22.5 miles per hour is higher than would be expected for a reasonable flight condition when comparison is made with similar helicopter flight attitudes. The data, however, are thought to be indicative of the trends to be expected at low forward speeds.

The large increase in lift of the model due to propeller operation in the static condition, which is essentially the thrust of the propellers, is further increased about 10 percent by the addition of the low forward speed (fig. 21(b)). It is significant to note that this increase in thrust at constant power with forward speed is very similar to that experienced by the helicopter rotor because of the lower induced losses that occur in the transition from hovering to forward flight.

No data were obtained from the simulated descent tests at angles of attack of 150°, 165°, and 180° because of the dangerous oscillations encountered; this oscillatory condition may have been the result of the interaction between the propeller slipstream and the velocity of descent. This conclusion appears to be substantiated, in part at least, by the tests with the propellers removed in which no evidence of such oscillations existed. It should be pointed out, however, that for an actual flight condition the velocity of descent would be much smaller than the value of 22 miles per hour at which the tests were made.

Stability-flap effectiveness.- Although the stability flap was found to be useful as a trimming device at the lower angles of attack, an investigation of the flap effectiveness was more important in the transition range where large negative pitching moments were measured with articulated-propeller operation. The variations of C_m, C_L, C_{h_a}, and C_{h_f} with δ_a are given in figure 22 for angles of attack of 41°, 46°, 58°, and 69° with articulated propellers operating for conditions of $C_{D_R} = 0$. For these tests, the ailavators were set at the maximum deflection of -48° inasmuch as the ailavator-effectiveness tests indicated that the model could not be trimmed with ailavators alone. However, with the ailavators set at -48° the stability flaps also could not trim out all of the negative pitching moment. The flap effectiveness is essentially constant throughout the deflection range and $\left(C_{m_\delta}\right)_f$ measured at $\delta_f = 0°$ is -0.0026, -0.0020, -0.0013, and -0.0017 per degree for angles of attack of 41°, 46°, 58°, and 69°, respectively. As compared with the flap effectiveness at an angle of attack of 29.0°, the flap effectiveness is not appreciably reduced at the higher angles of

attack. The slope $\left(C_{h_\delta}\right)_f$ measured at $\delta_f = 0^\circ$ is essentially constant at -0.0075 per degree for all the conditions tested except for an angle of attack of 69°. The slope for an angle of attack of 69° increased gradually with flap deflection from 24° to -4° with a value at $\delta_f = 0^\circ$ of -0.0103 per degree. For flap deflections from -8° to 16° a reversal in slope is shown. Apparently up to very high attitudes the stability flaps, when deflected, do not influence the flow over the ailavators because the ailavator hinge moments remained unchanged for the stability-flap tests. At the highest attitude investigated ($\alpha \approx 69^\circ$) some interaction interference is shown by large increases in the ailavator hinge moments when the stability-flap hinge moments reversed.

SUMMARY OF RESULTS

The results of an investigation of the static longitudinal stability and control of a convertible-type airplane as affected by articulated- and by rigid-propeller operation showed the following:

(1) The destabilizing effect of propeller operation was more pronounced for rigid-propeller operation than for articulated-propeller operation because of the reduction in propeller normal force and the increment of positive pitching moment due to propeller articulation.

(2) The airplane for full-power operation has a positive-static-margin average of about 5 percent for articulated-propeller operation and about 3 percent for rigid-propeller operation over most of the lift-coefficient range from 0.50 (11.3° angle of attack) to about 1.90 (29.0° angle of attack). At a lift coefficient of about 1.90, however, no appreciable difference in the stick-fixed stability between the two modes of propeller operation is present.

(3) The all-movable horizontal tail is sufficiently powerful to trim the airplane throughout the lift-coefficient range (from 0.50 to 1.80) for full-power operation. Appreciably less ailavator deflection is required for trim for rigid-propeller operation with the difference in the high-lift-coefficient range amounting to about 14° which is about one-half the deflection required for articulated-propeller operation.

(4) The slope of the ailavator hinge-moment curve against deflection (for full-power operation) showed a reversal from positive to negative values at low lift coefficients and then gradually decreased negatively with increasing lift coefficient.

(5) The ailavator effectiveness, for articulated-propeller operation at full power, increased from -0.0050 per degree at a lift

coefficient of 0.48 (11.3° angle of attack) to -0.0092 per degree at a lift coefficient of 1.84 (29.0° angle of attack). For rigid-propeller operation, however, the ailavator effectiveness was essentially constant at a value of -0.0057 per degree throughout the lift-coefficient range as compared to the propellers-removed value of about -0.0050.

(6) Full-power operation for articulated- and rigid-propeller operation increased the slope of the lift curve to about 0.068 and 0.070 per degree, respectively, as compared to the value of 0.032 per degree obtained with propellers removed.

(7) The airplane can be trimmed with the ailavators alone in the high-angle-of-attack range up to 58° for rigid-propeller operation. No trim point, however, is indicated for any of the conditions for articulated-propeller operation.

(8) The results of the ailavator-effectiveness tests show that the ailavators have a high degree of effectiveness for the zero-velocity condition. For the condition at an angle of attack of 90° with a forward velocity of 22.5 miles per hour, the data indicate that very little, if any, of the propeller slipstream passes over the tail; however, the forward velocity is appreciably larger than would be expected for an actual flight condition.

(9) The stability flap can be used as a trimming device for the normal-flight attitudes; however, in the transition range the effectiveness is insufficient for trimming.

Langley Aeronautical Laboratory
National Advisory Committee for Aeronautics
Langley Air Force Base, Va., March 10, 1949

REFERENCES

1. Lange, Roy H., Cocke, Bennie W., Jr., and Proterra, Anthony J.: Preliminary Full-Scale Investigation of a $\frac{1}{3}$-Scale Model of a Convertible-Type Airplane. NACA RM L9C29, 1949.

2. Schuldenfrei, Marvin: Some Notes on the Determination of the Stick-Fixed Neutral Point from Wind-Tunnel Data. NACA RB 3I20, 1943.

3. Goett, Harry J., and Pass, H. R.: Effect of Propeller Operation on the Pitching Moments of Single-Engine Monoplanes. NACA ACR, May 1941.

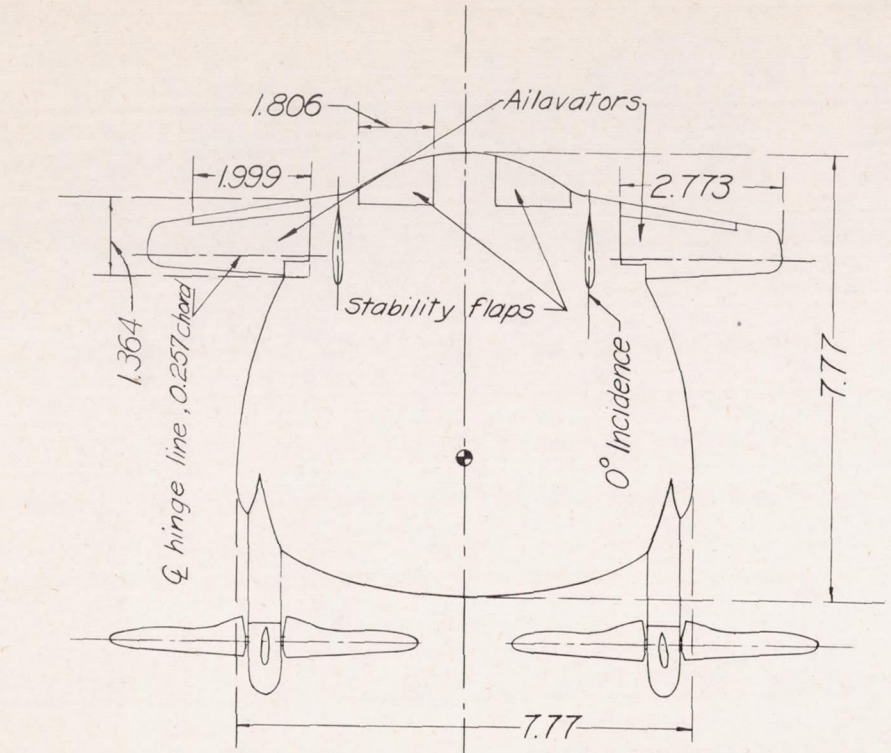

Geometric characteristics

Aspect ratio	1.27
Areas, sq ft:	
Wing (including stability flap)	47.444
Stability flaps (two)	1.671
All-movable horizontal tail (two ailavators)	5.578
Vertical tails (two)	3.158
Horizontal tail tab (one)	0.338
Lengths, ft:	
Span	7.777
Mean aerodynamic chord	6.611
Airfoil sections:	
Wing	NACA 0016
Horizontal tail	
Root	NACA 0015
Tip	NACA 0009
Vertical tail	12-percent thick, symmetrical

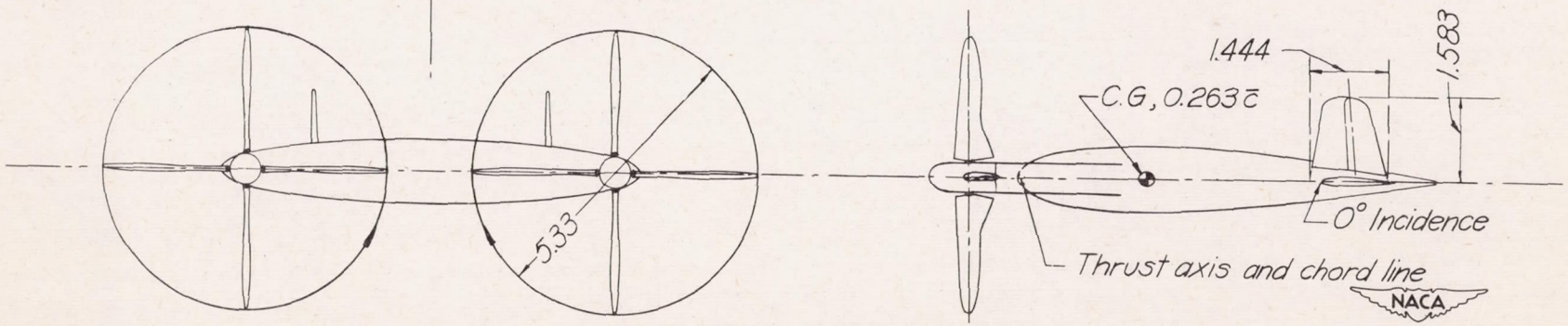

Figure 1.— General arrangement of the model. (All dimensions are given in ft.)

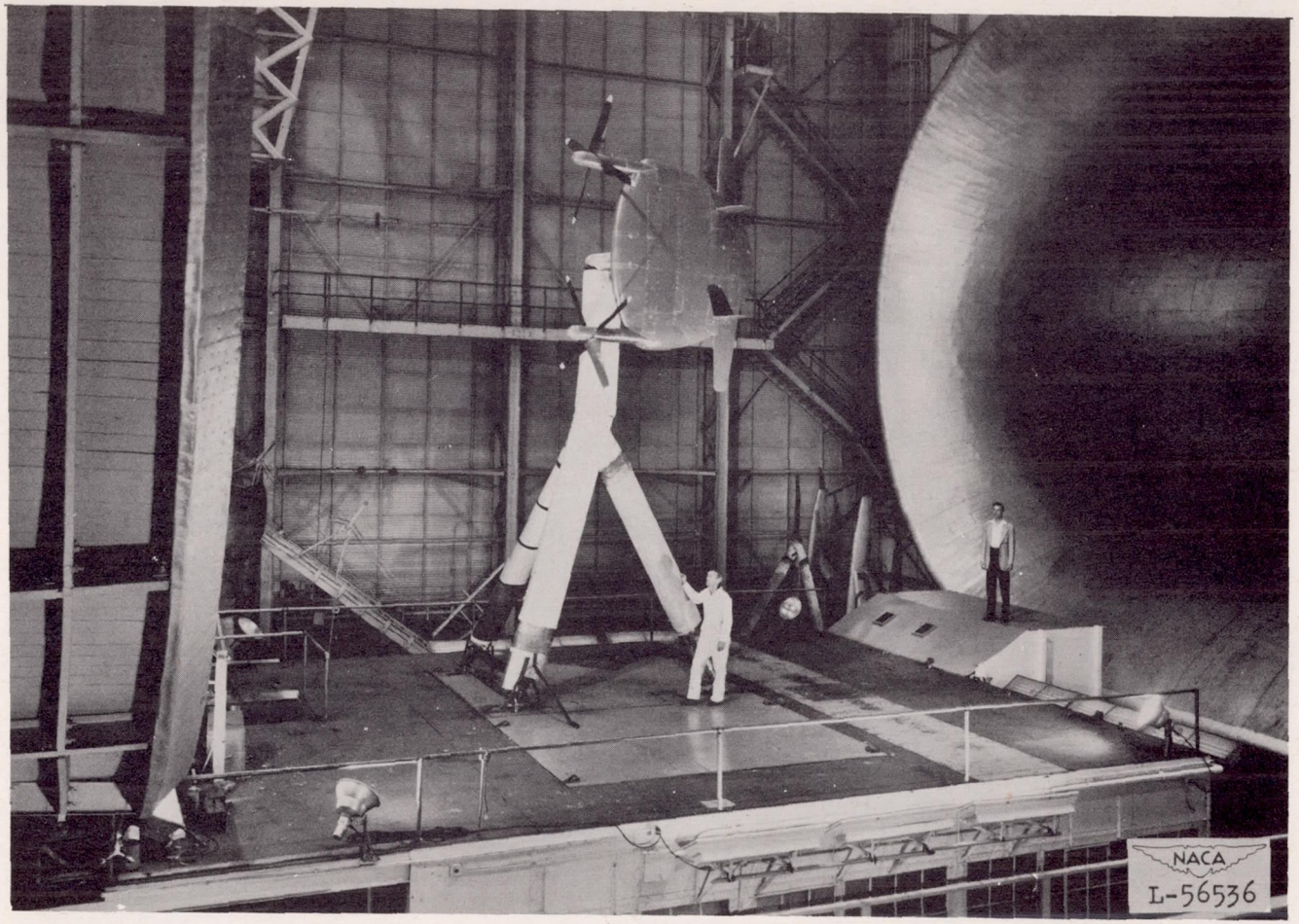

(a) Three-fourth front view.

Figure 2.- A $\frac{1}{3}$-scale model of a convertible-type airplane mounted sidewise for tests in the Langley full-scale tunnel.

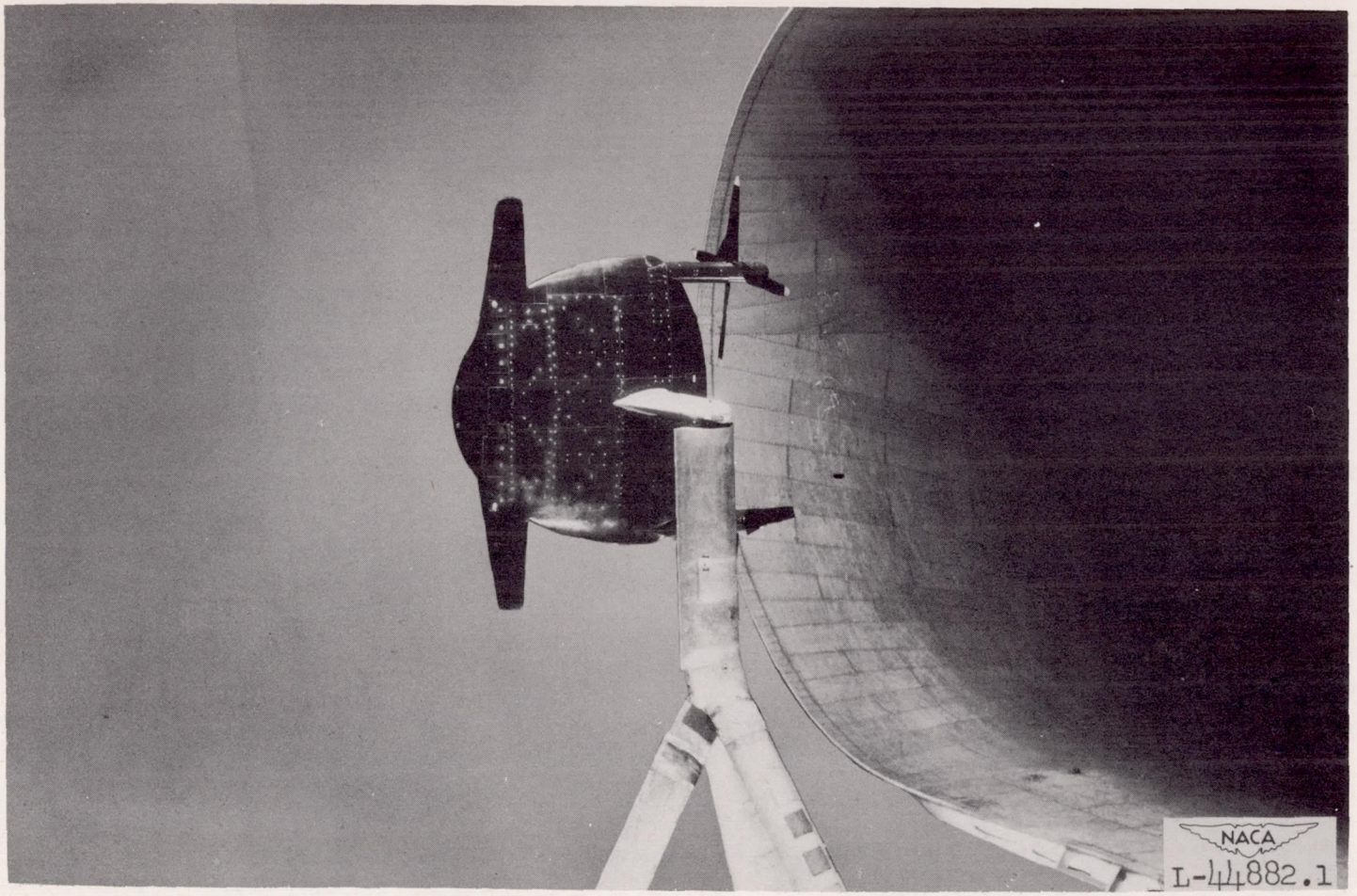

(b) Three-fourth rear view.

Figure 2.- Continued.

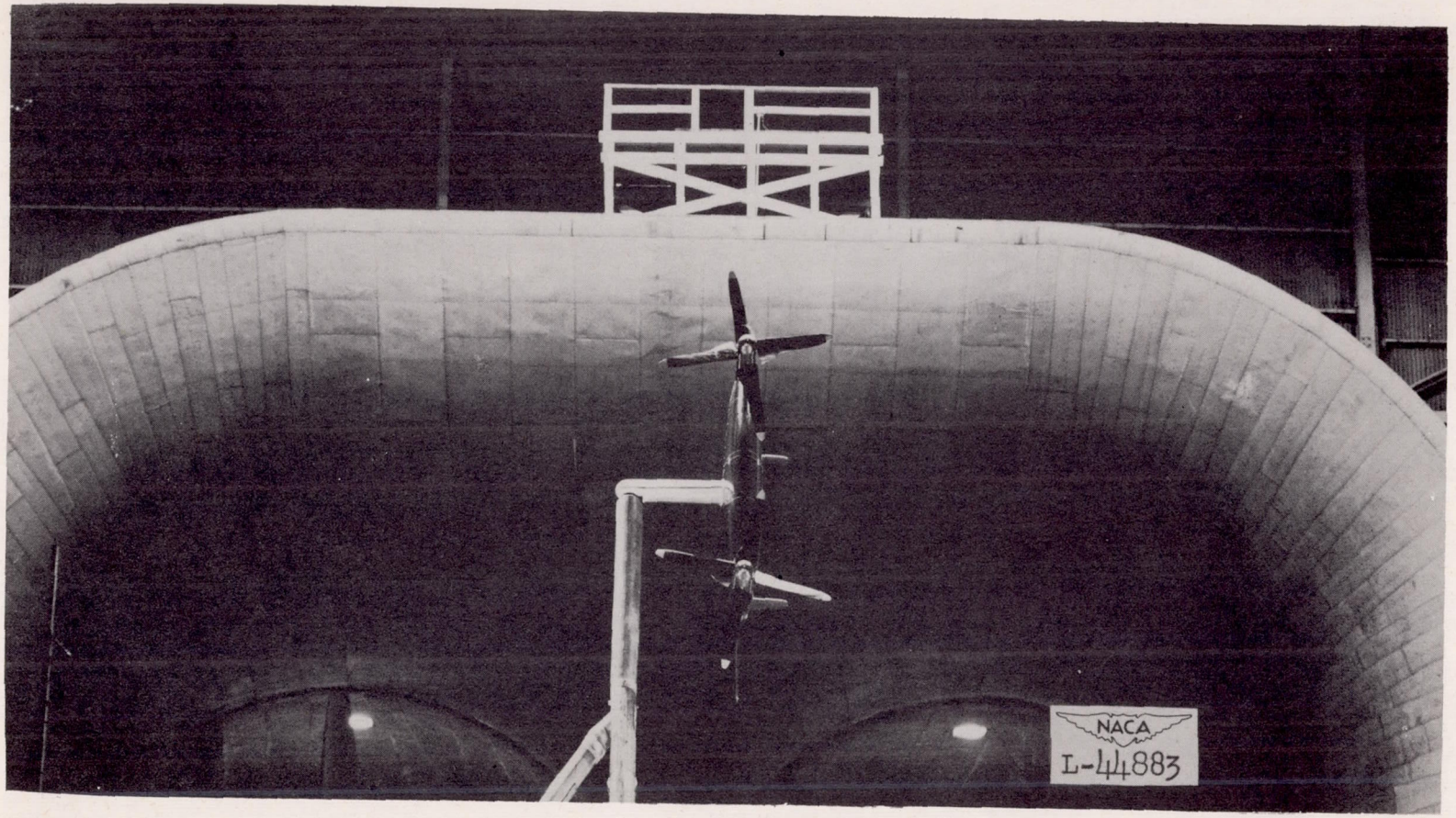

(c) Front view.

Figure 2.– Concluded.

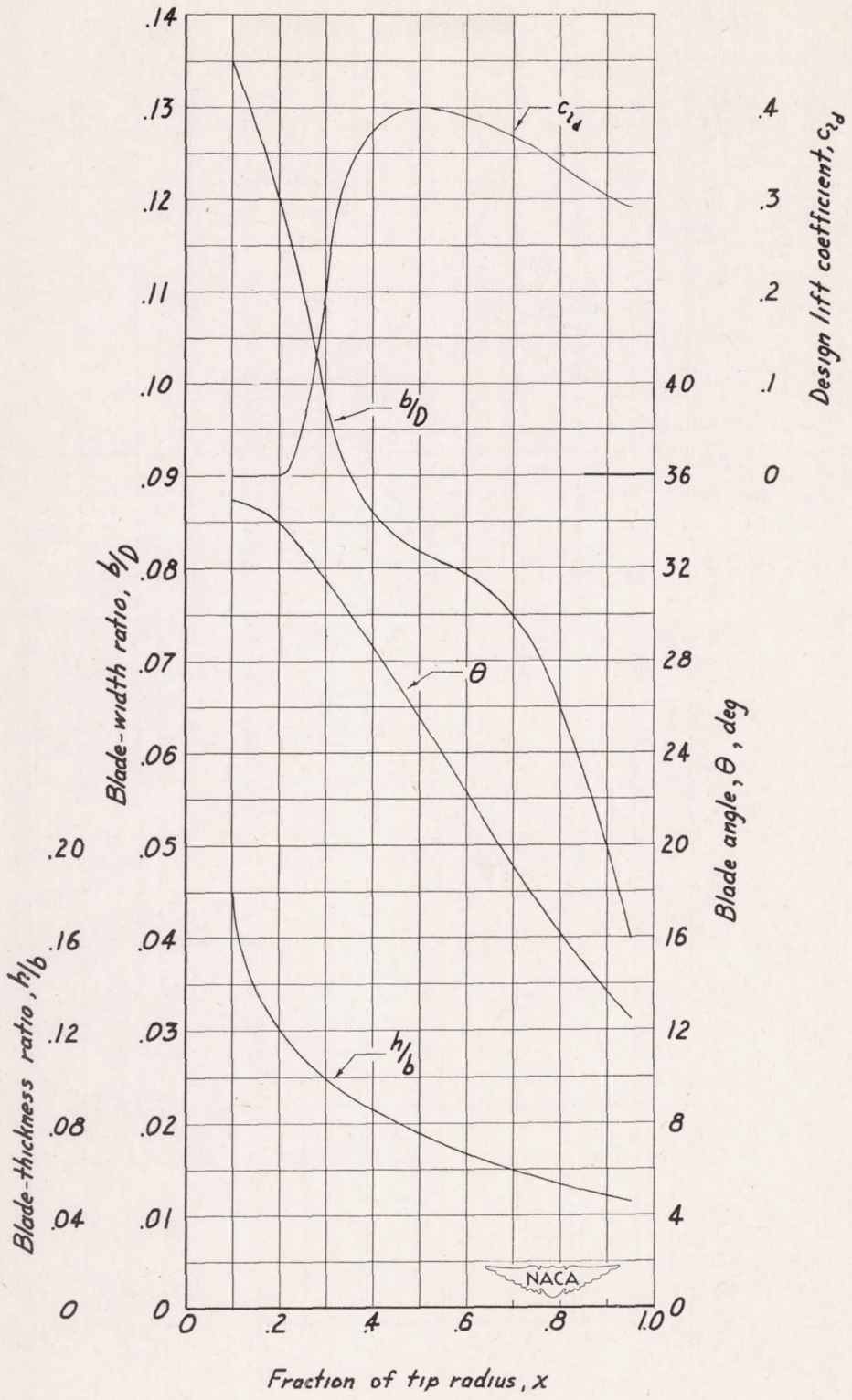

Figure 3.- Blade-form curves for the model propeller.

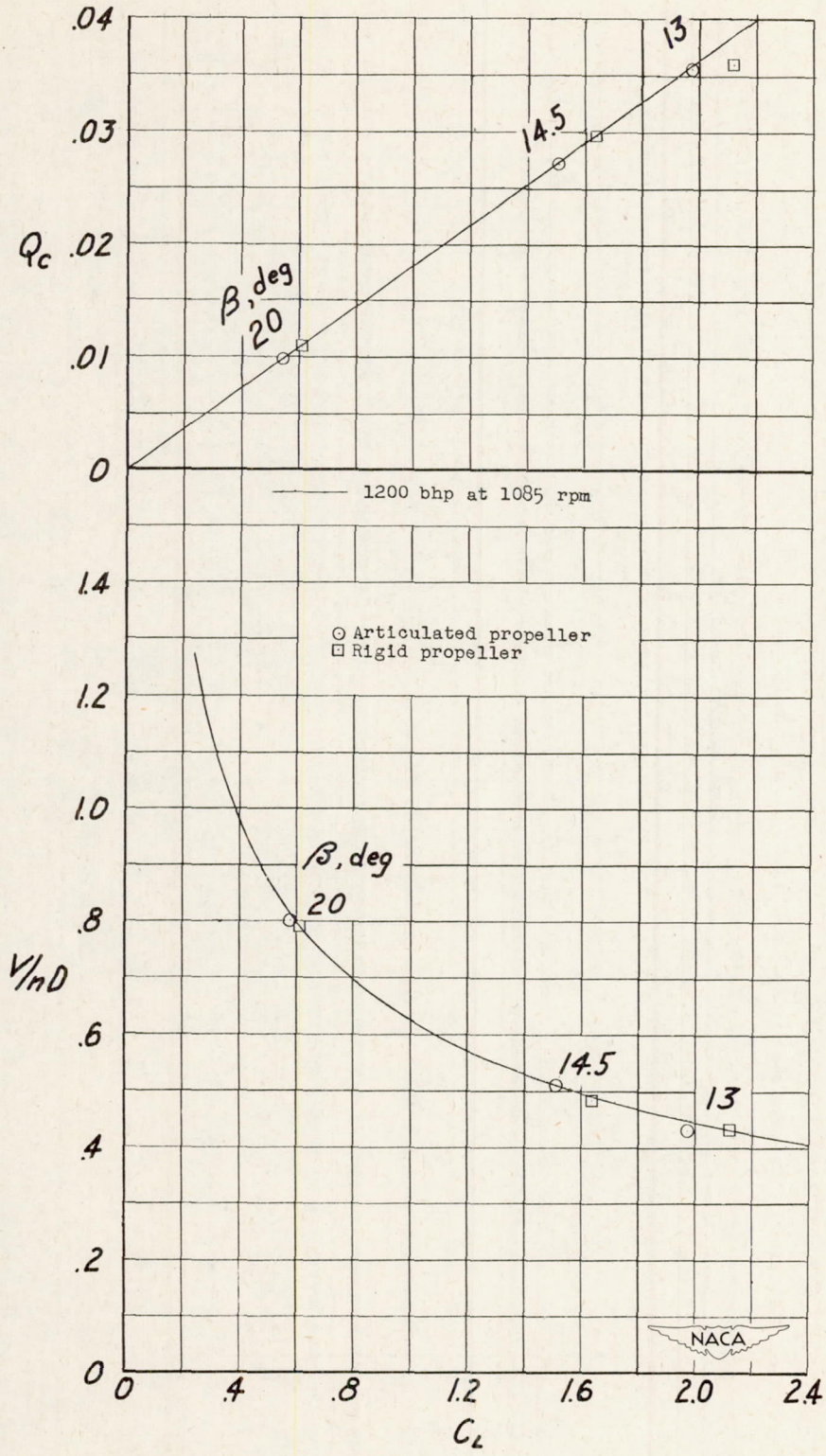

Figure 4.- Variation of Q_c and V/nD with C_L for simulated full-power operation at sea level.

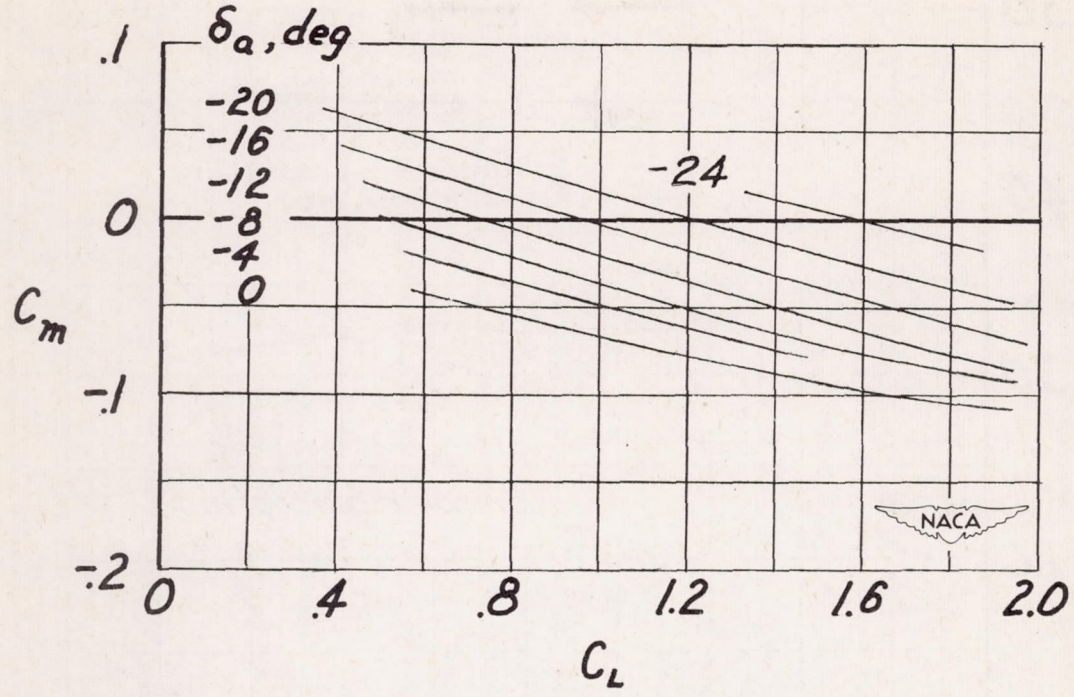

(a) Articulated propellers.

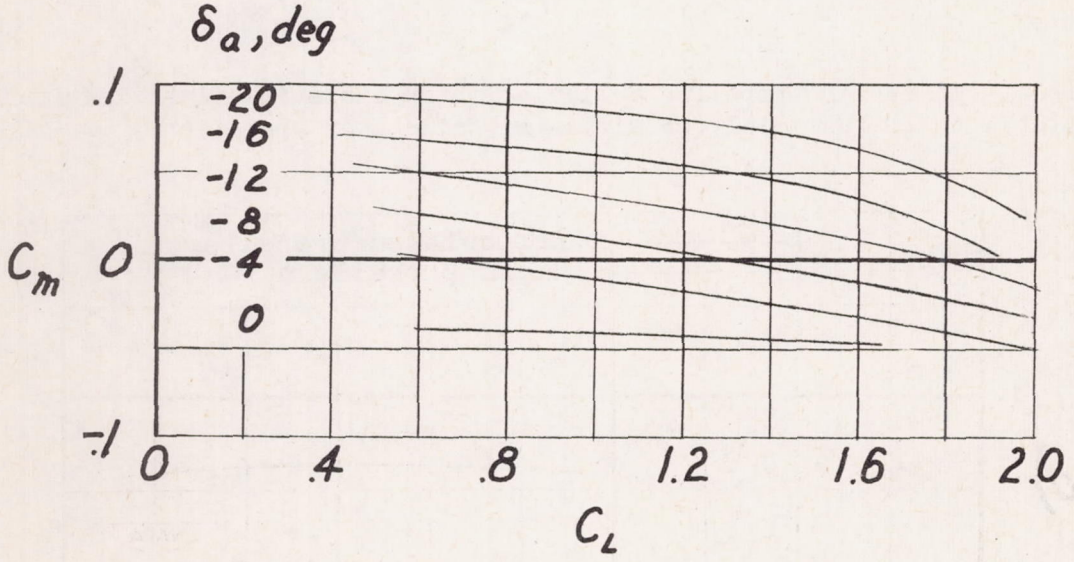

(b) Rigid propellers.

Figure 5.- Variation of C_m with C_L for several ailavator deflections for simulated full-power operation. $\delta_f = 0^\circ$.

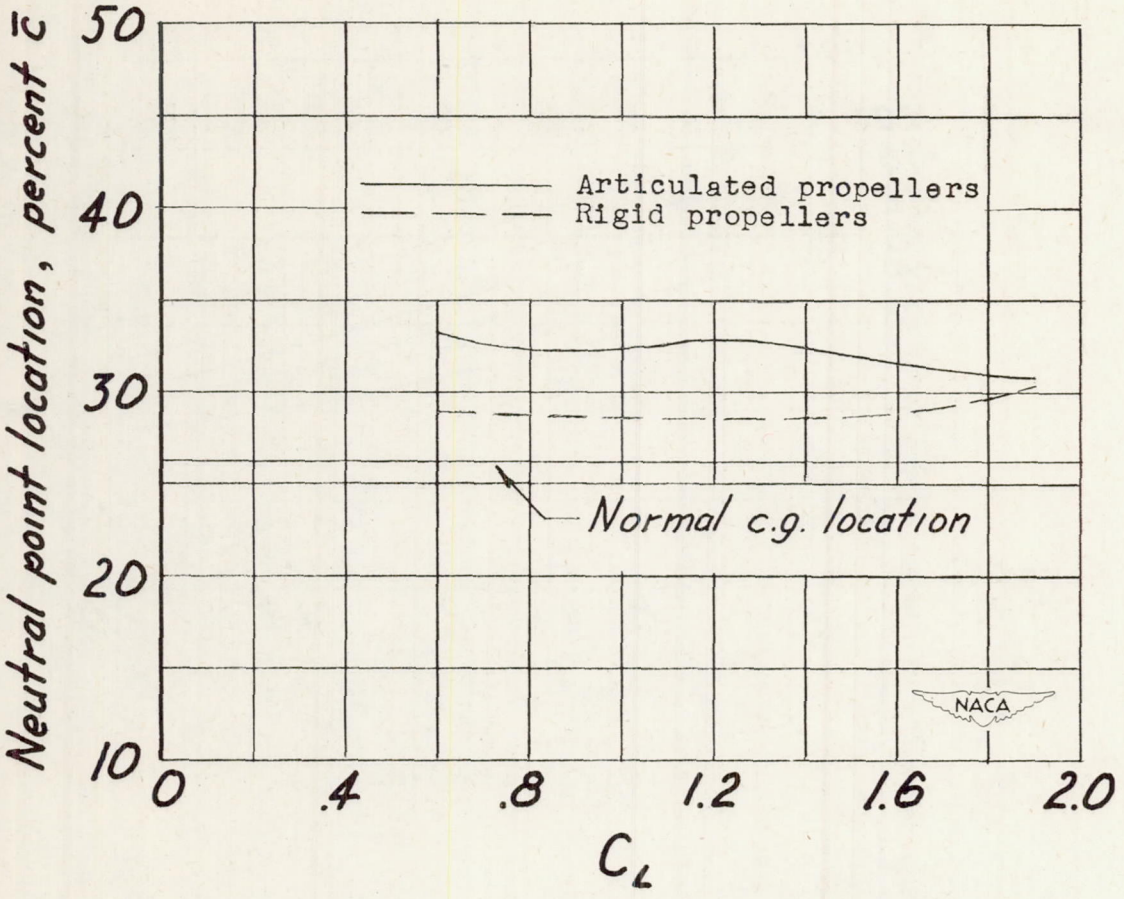

Figure 6.– Effect of propeller articulation on the stick-fixed longitudinal stability of the model for simulated full-power operation. $\delta_f = 0^\circ$.

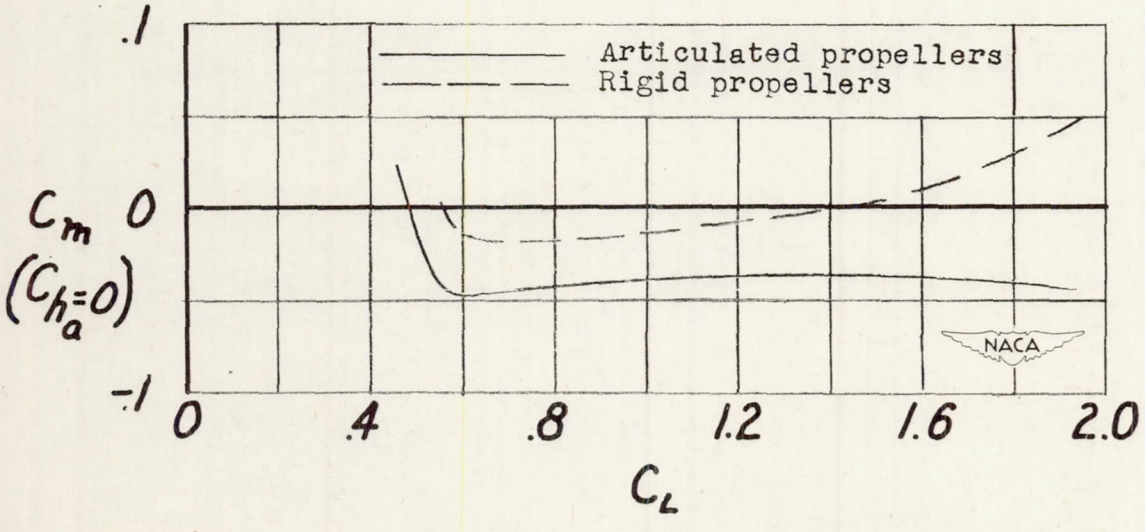

Figure 7.– Effect of propeller articulation on the variation of C_m with C_L for simulated full-power operation. $\delta_f = 0^\circ$.

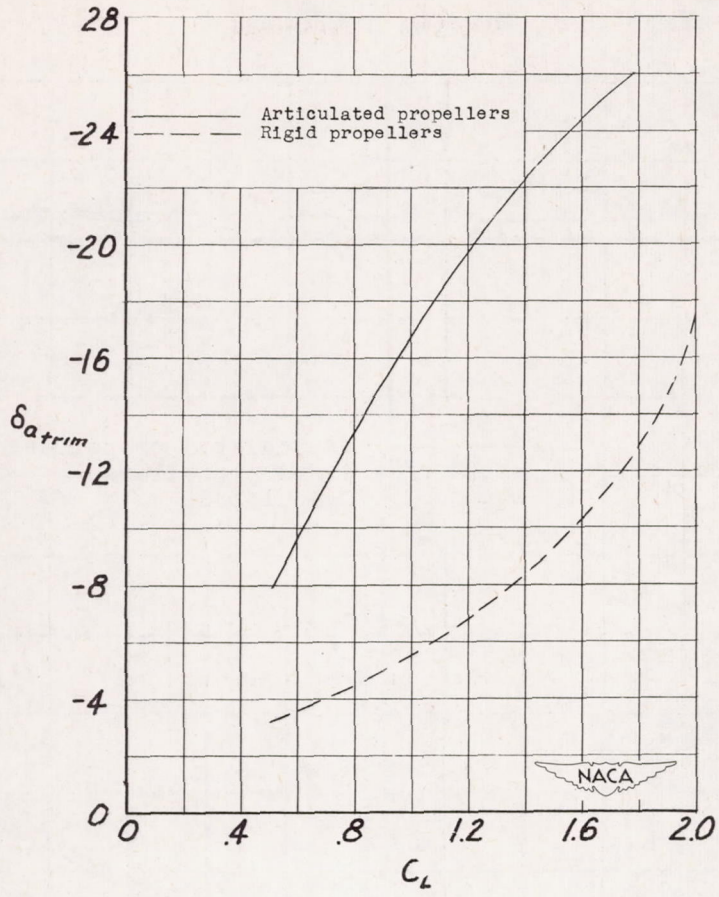

Figure 8.– Effect of propeller articulation on the variation of ailavator deflection required for trim with lift coefficient for simulated full-power operation. $\delta_f = 0^\circ$.

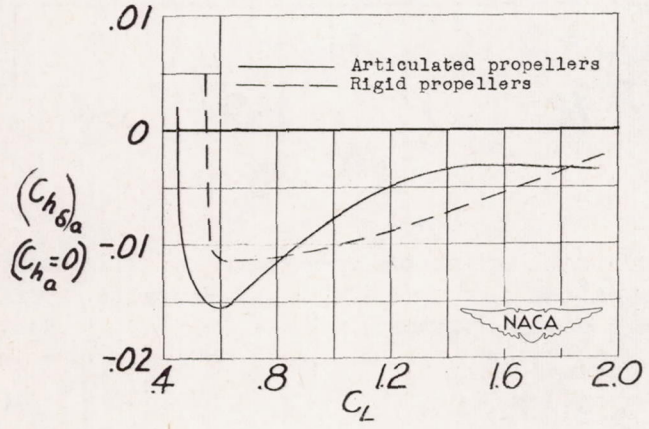

Figure 9.– Effect of propeller articulation on the variation of $C_{h_{\delta_a}}$ with C_L for simulated full-power operation. $\delta_f = 0^\circ$.

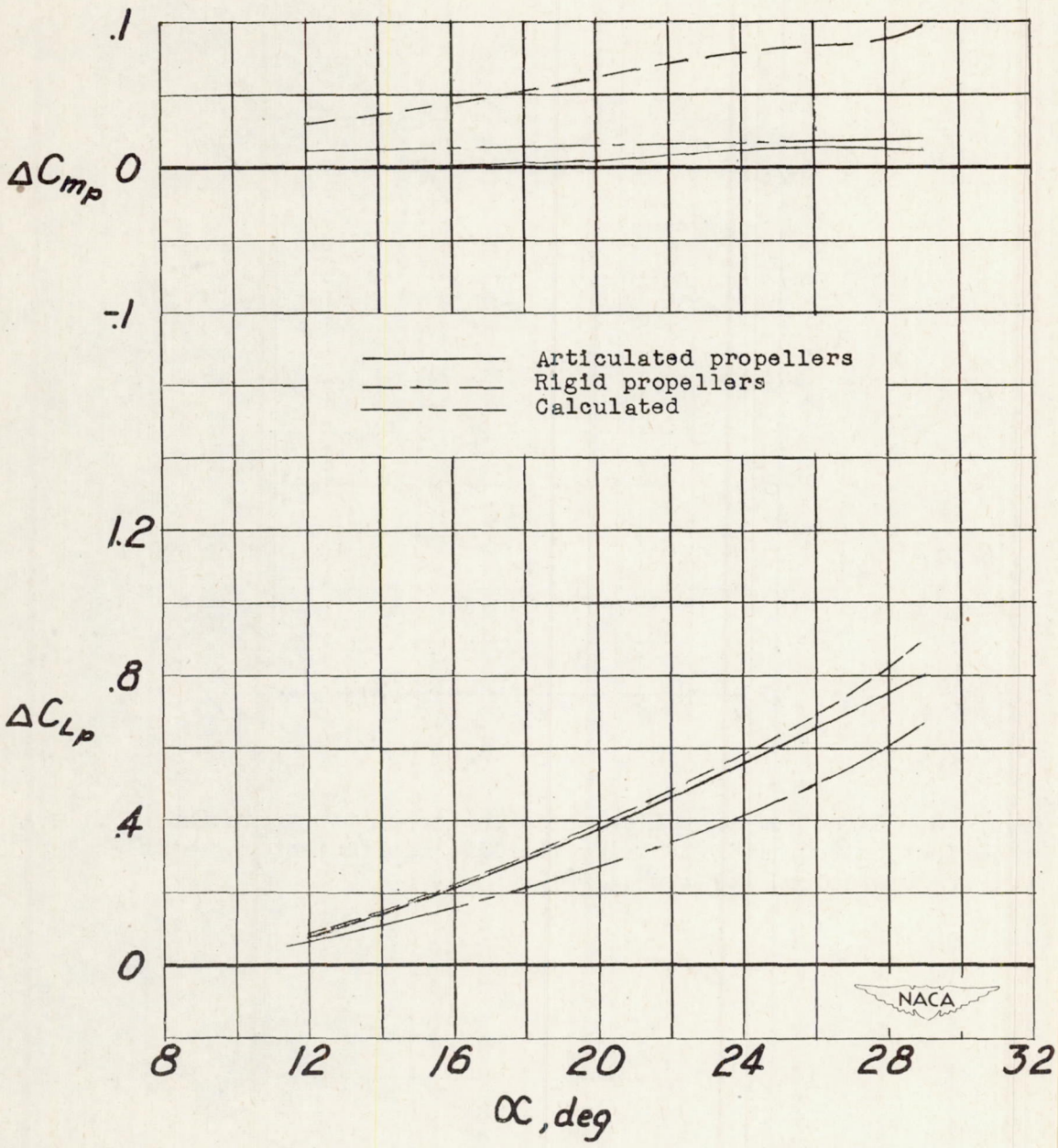

Figure 10.- Increments of pitching-moment and lift coefficients due to propeller operation for model with all-movable horizontal tail removed. Full-power operation; $\delta_f = 0^\circ$.

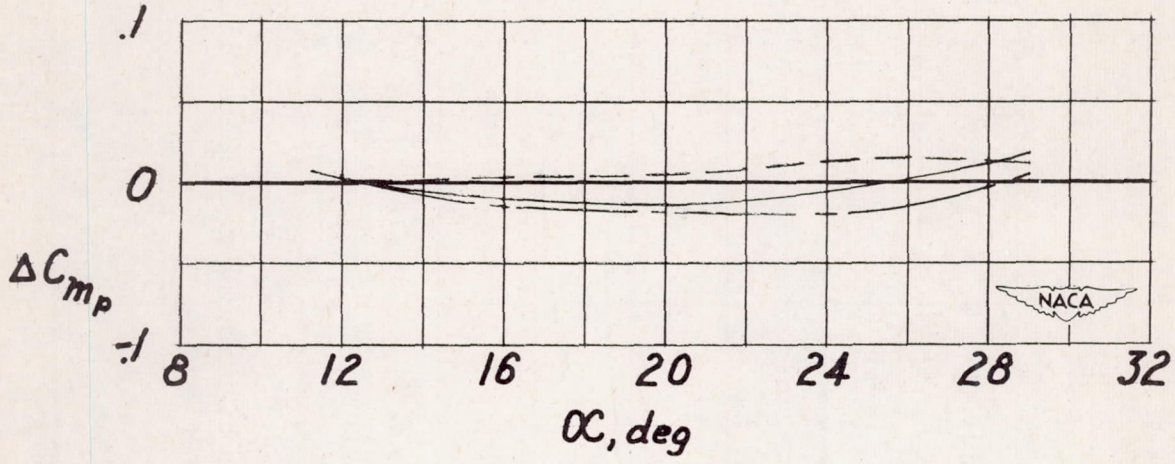

(a) Articulated propellers.

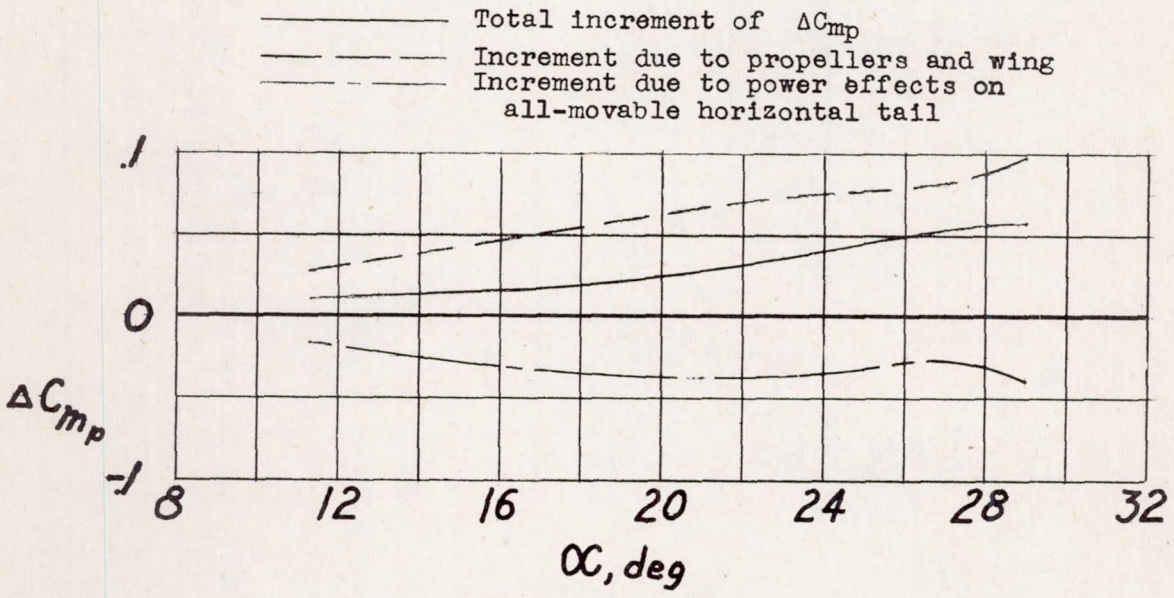

(b) Rigid propellers.

Figure 11.- Increments of pitching-moment coefficients due to propeller operation. Full-power operation; $\delta_f = 0^\circ$.

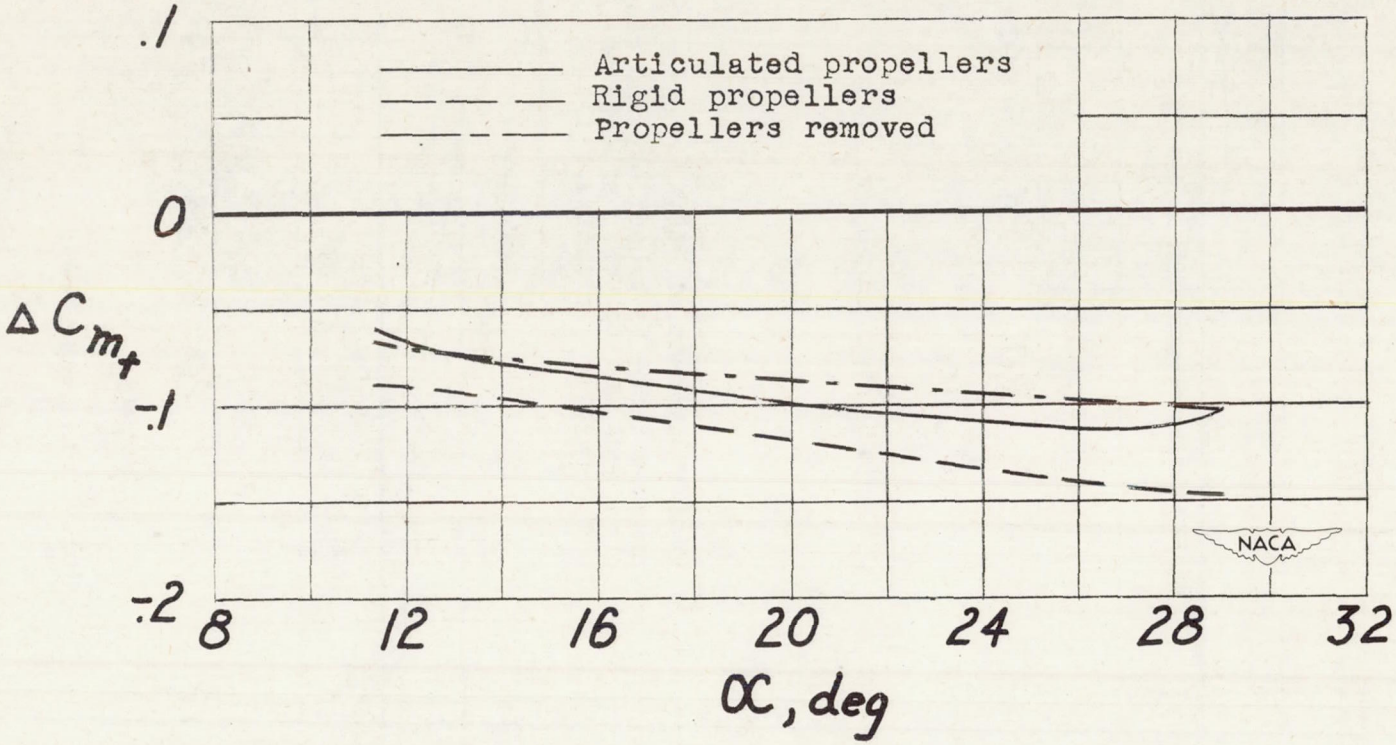

Figure 12.– Effect of full–power operation on the total increment of pitching–moment coefficient due to the all–movable horizontal tail. $\delta_f = 0^\circ$.

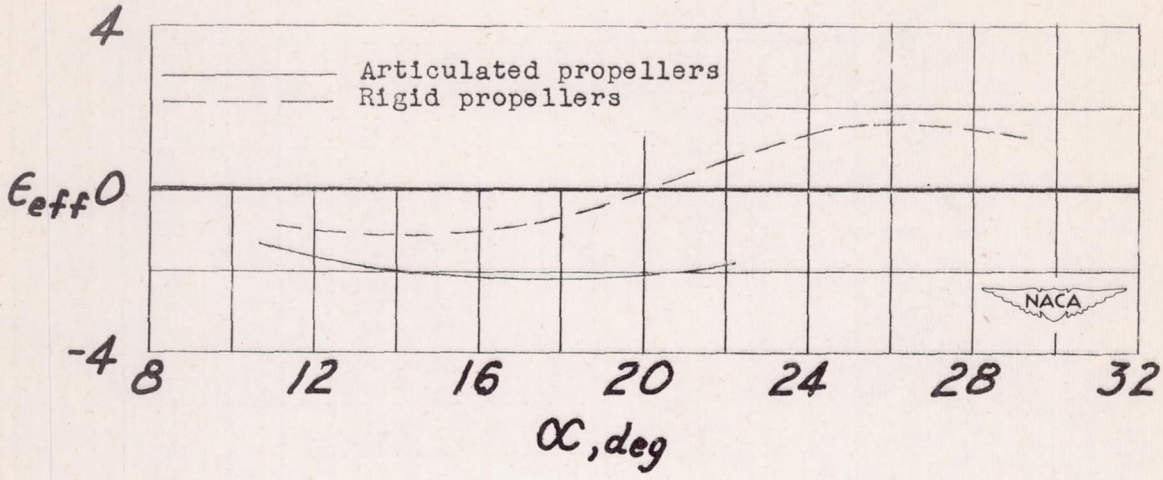

Figure 13.- Effect of propeller articulation on the variation of ϵ_{eff} with α for simulated full-power operation. $\delta_f = 0^\circ$.

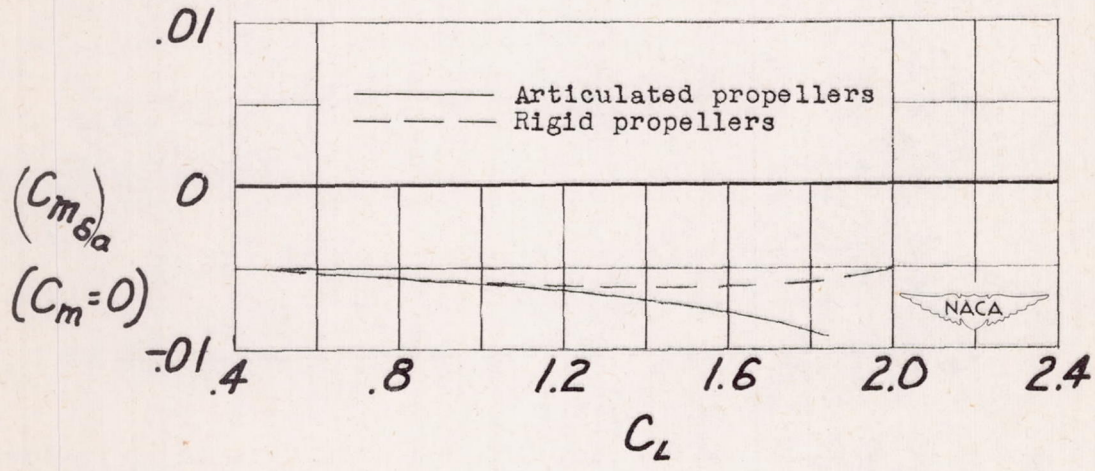

Figure 14.- Effect of propeller articulation on the variation of $(C_{m_\delta})_a$ with C_L for simulated full-power operation. $\delta_f = 0^\circ$.

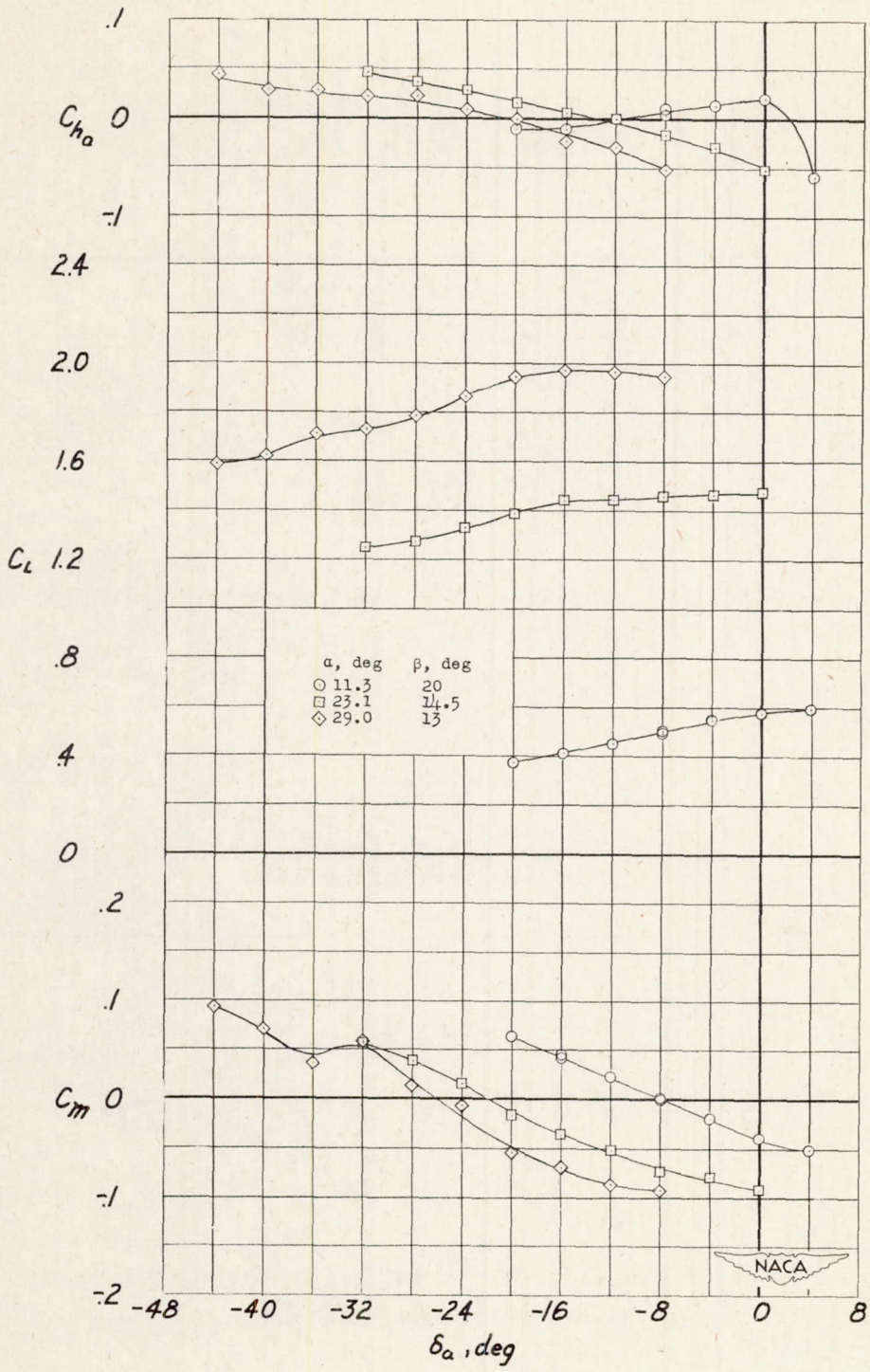

(a) Articulated propellers.

Figure 15.- Variation of C_m, C_L, and C_{h_a} with δ_a of the model for simulated full-power operation. $\delta_f = 0^\circ$.

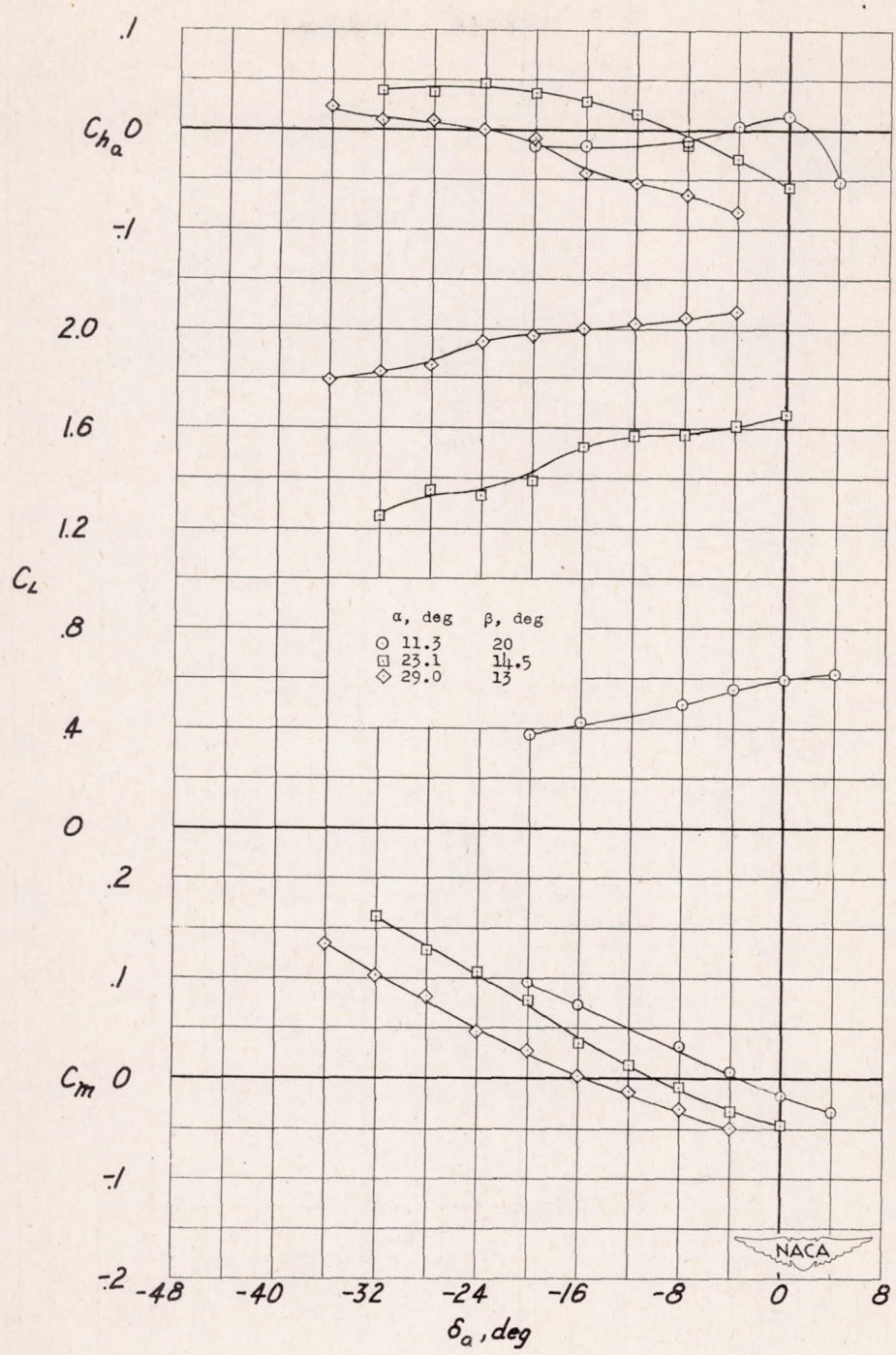

(b) Rigid propellers.

Figure 15.- Concluded.

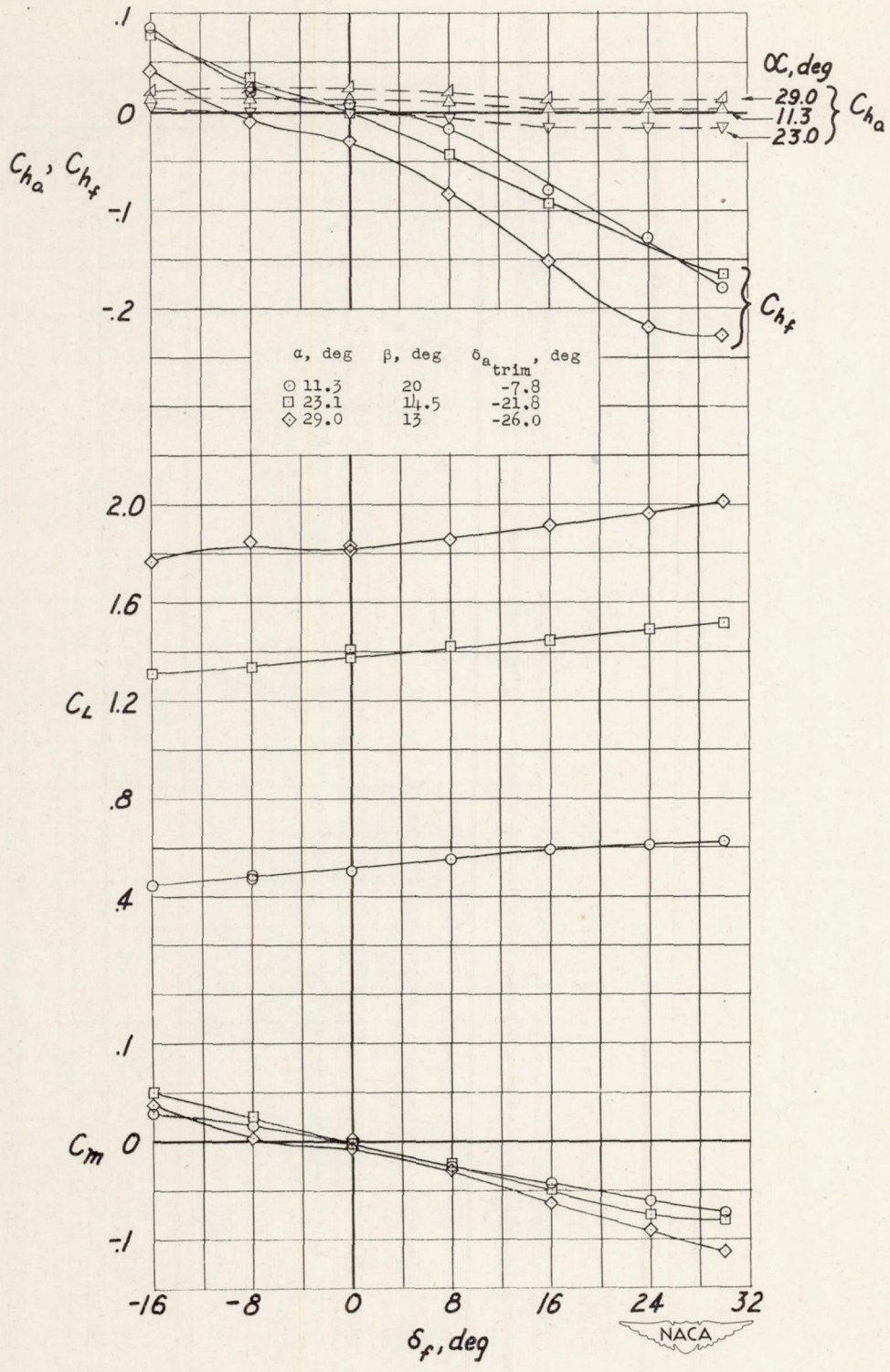

Figure 16.– Variation of C_m, C_L, C_{h_f}, and C_{h_a} with δ_f for simulated full–power operation with articulated propellers.

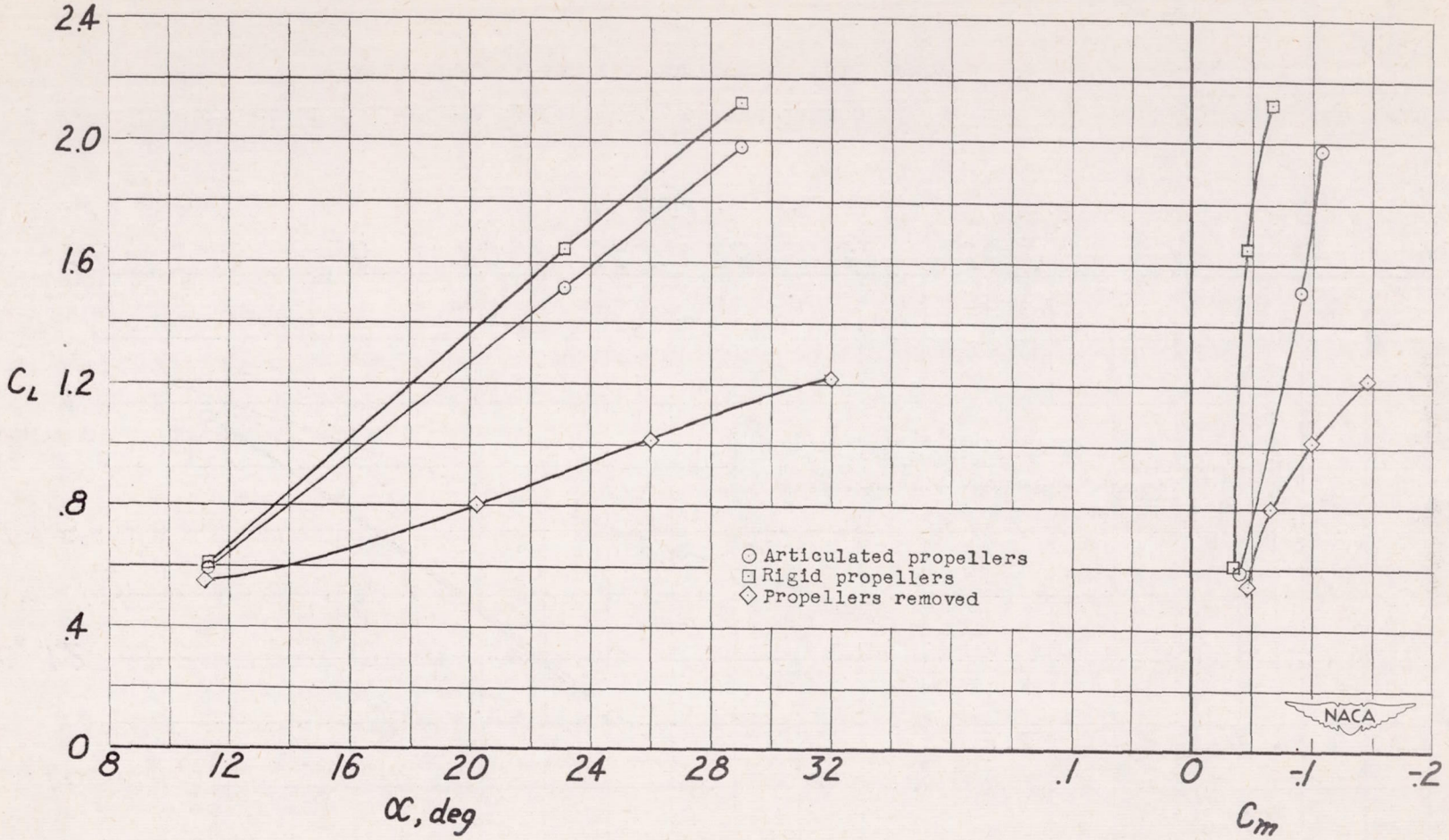

Figure 17.- Effect of full-power operation on the variation of α and C_m with C_L for the model with the all-movable horizontal tail installed. $\delta_f = 0^\circ$.

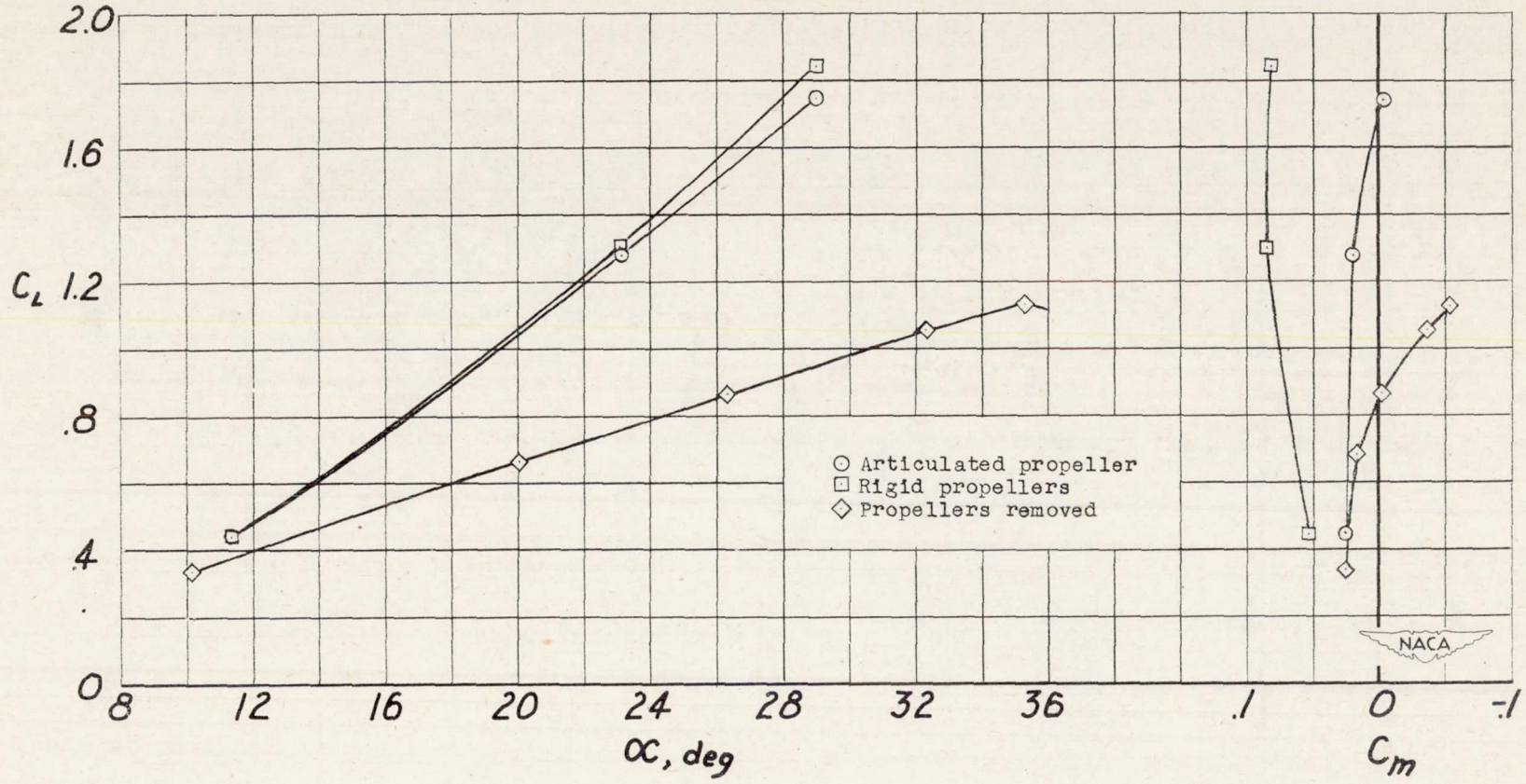

Figure 18.- Effect of full-power operation on the variation of α and C_m with C_L for the model with the all-movable horizontal tail removed; $\delta_f = 0^\circ$.

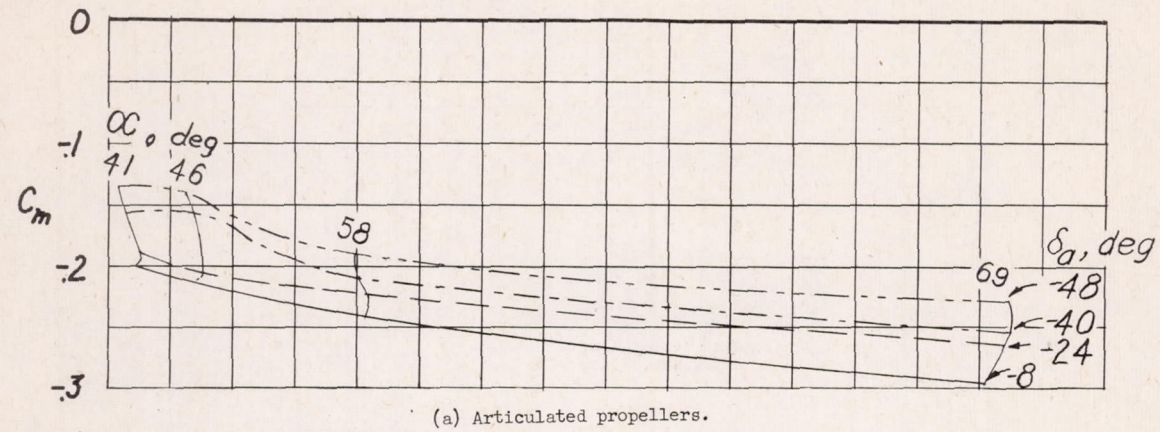

(a) Articulated propellers.

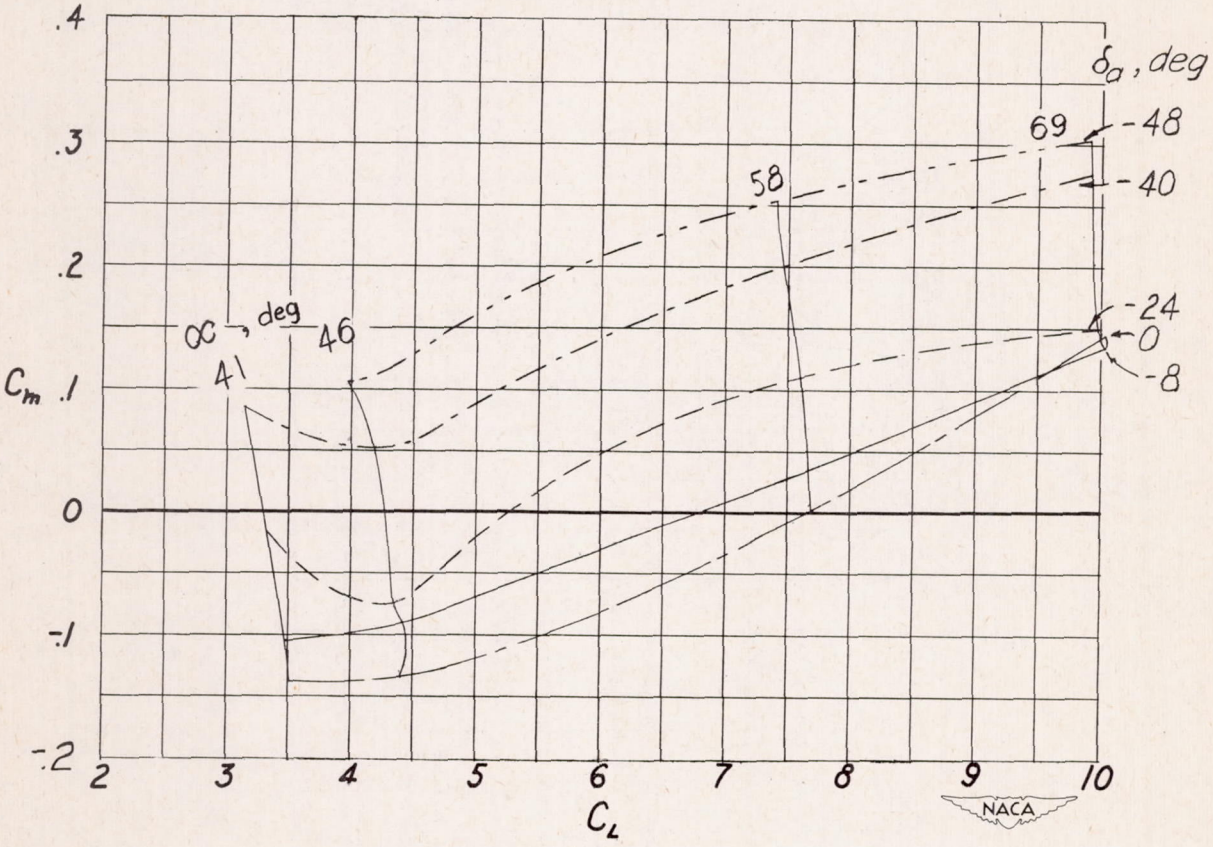

(b) Rigid propellers.

Figure 19.- Variation of C_m with C_L for several ailavator deflections. $C_{D_R} \approx 0$; $\delta_f = 0^\circ$.

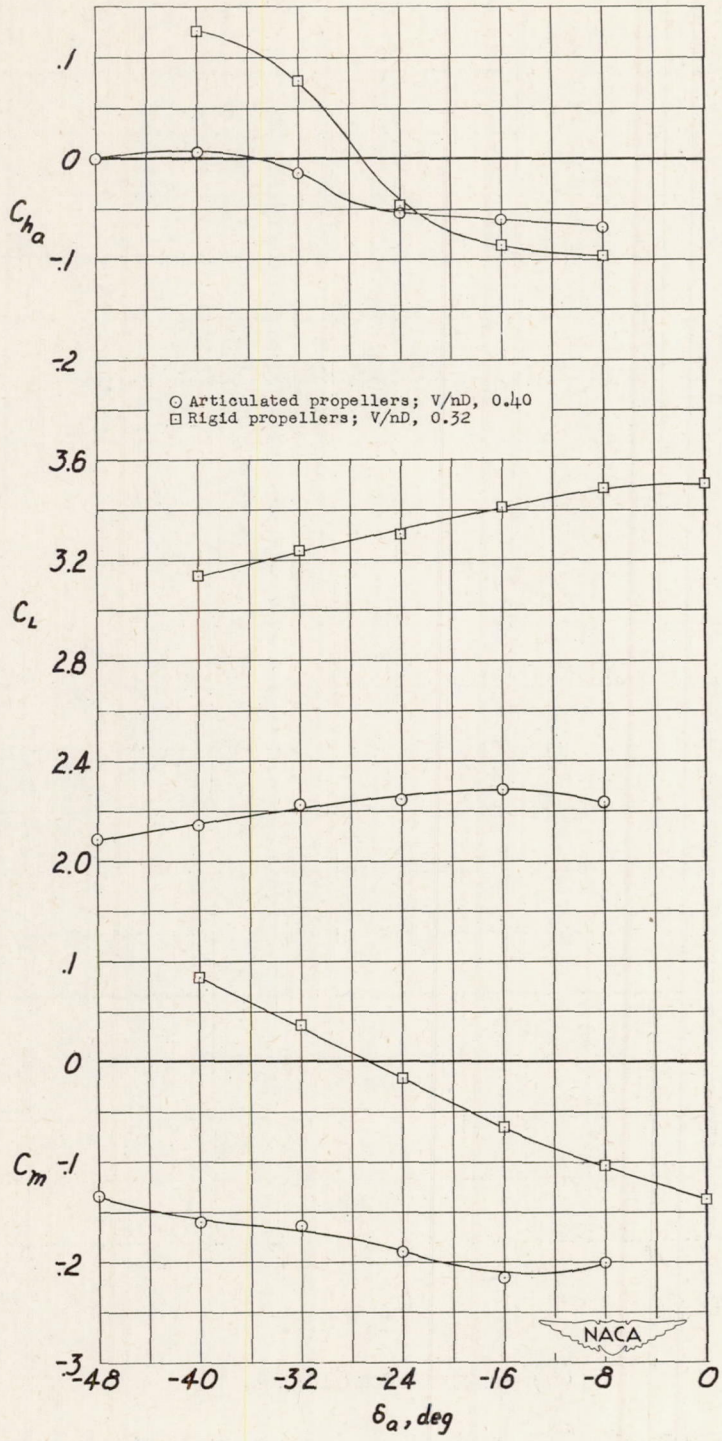

(a) $\alpha \approx 41^\circ$.

Figure 20.– Effect of propeller articulation on the variation of C_m, C_L, and C_{h_a} with δ_a for conditions of $C_{D_R} = 0$. $\beta = 11.5^\circ$; $\delta_f = 0^\circ$.

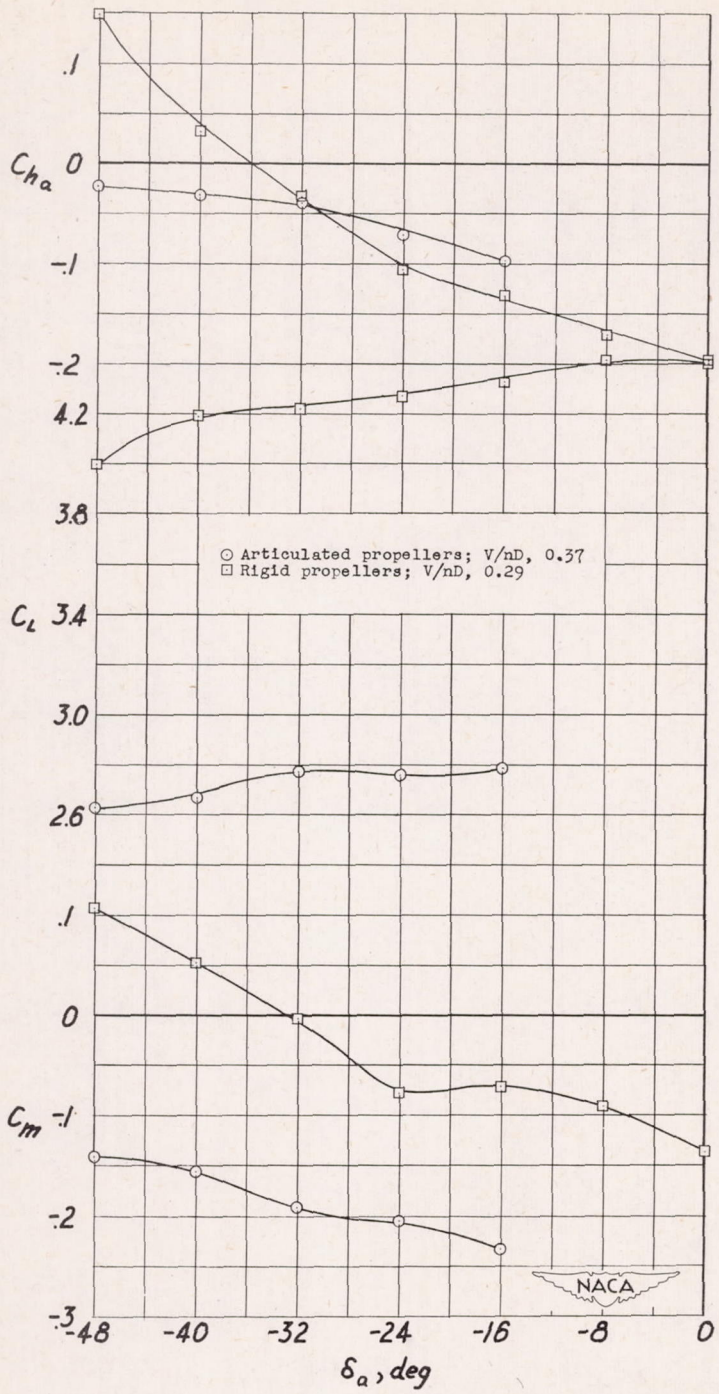

(b) $\alpha \approx 46^\circ$.

Figure 20.- Continued.

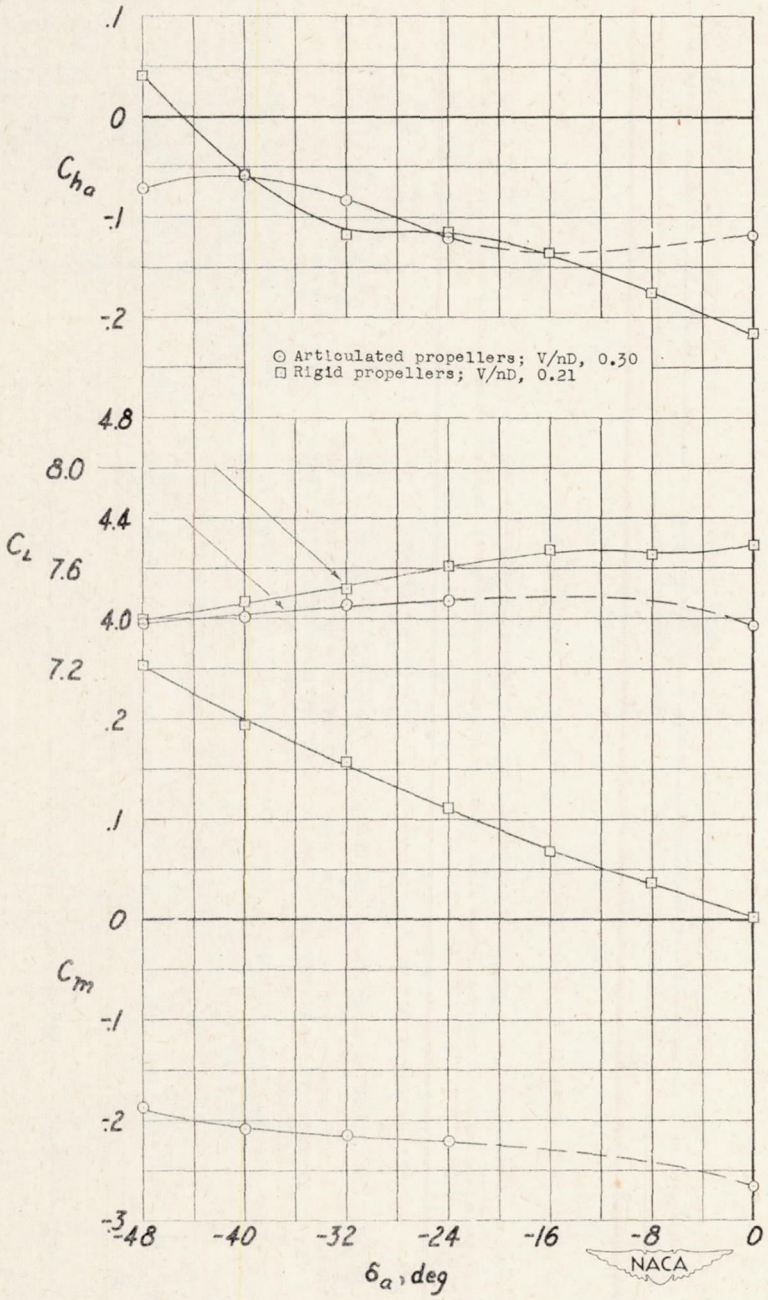

(c) $\alpha \approx 58°$.

Figure 20.- Continued.

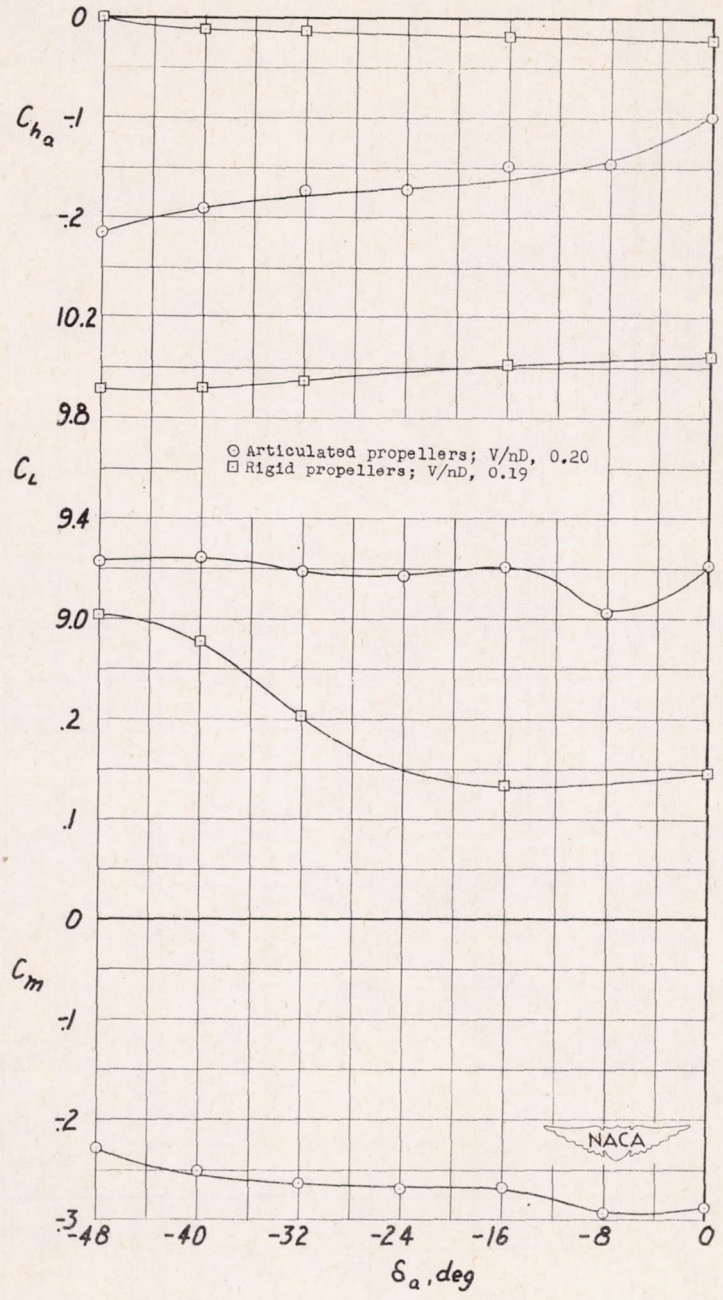

(d) $\alpha \approx 69^\circ$.

Figure 20.– Concluded.

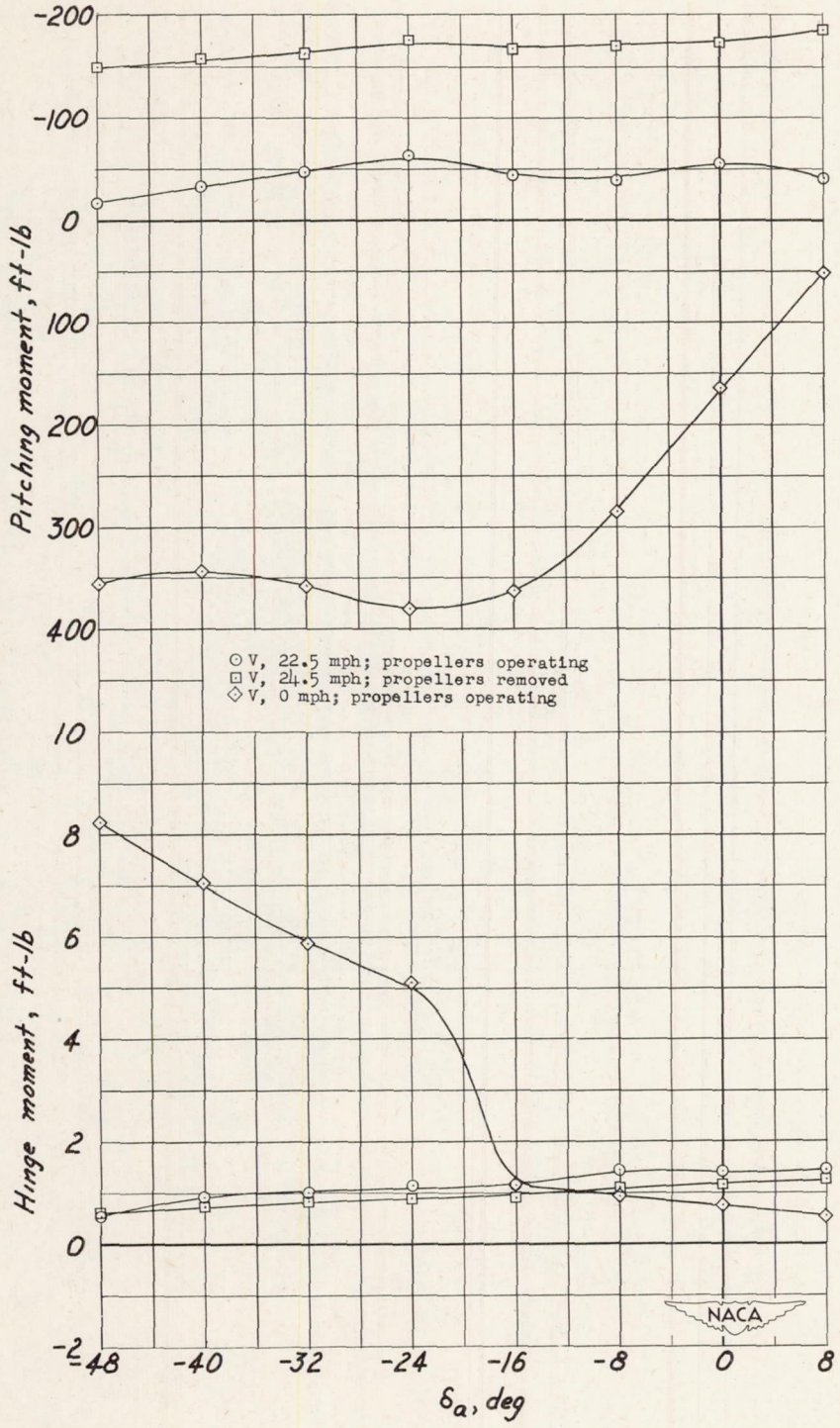

(a) Variation of pitching moment and hinge moment with δ_a.

Figure 21.- Effect of propeller operation and forward velocity on ailavator effectiveness. Articulated propellers; $\alpha_u = 90^\circ$; $\beta = 11.5^\circ$; 2500 rpm; $\delta_f = 0^\circ$.

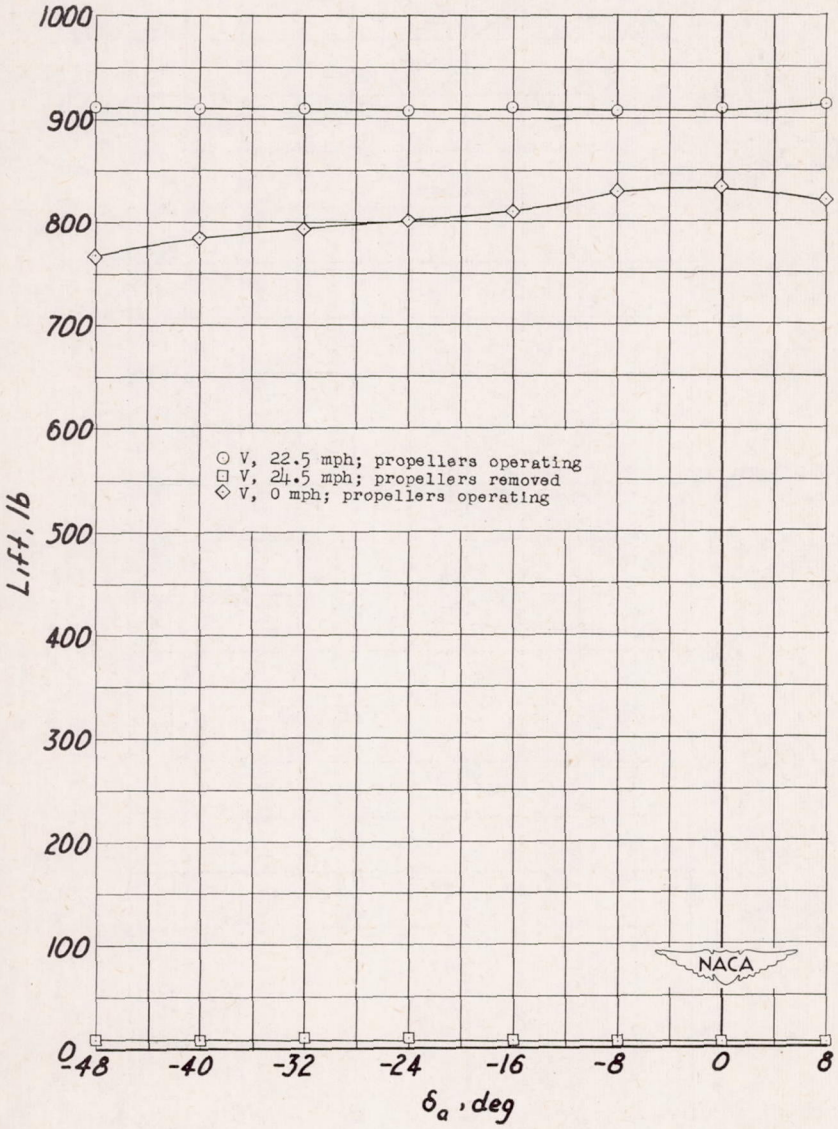

(b) Variation of lift with δ_a.

Figure 21.- Concluded.

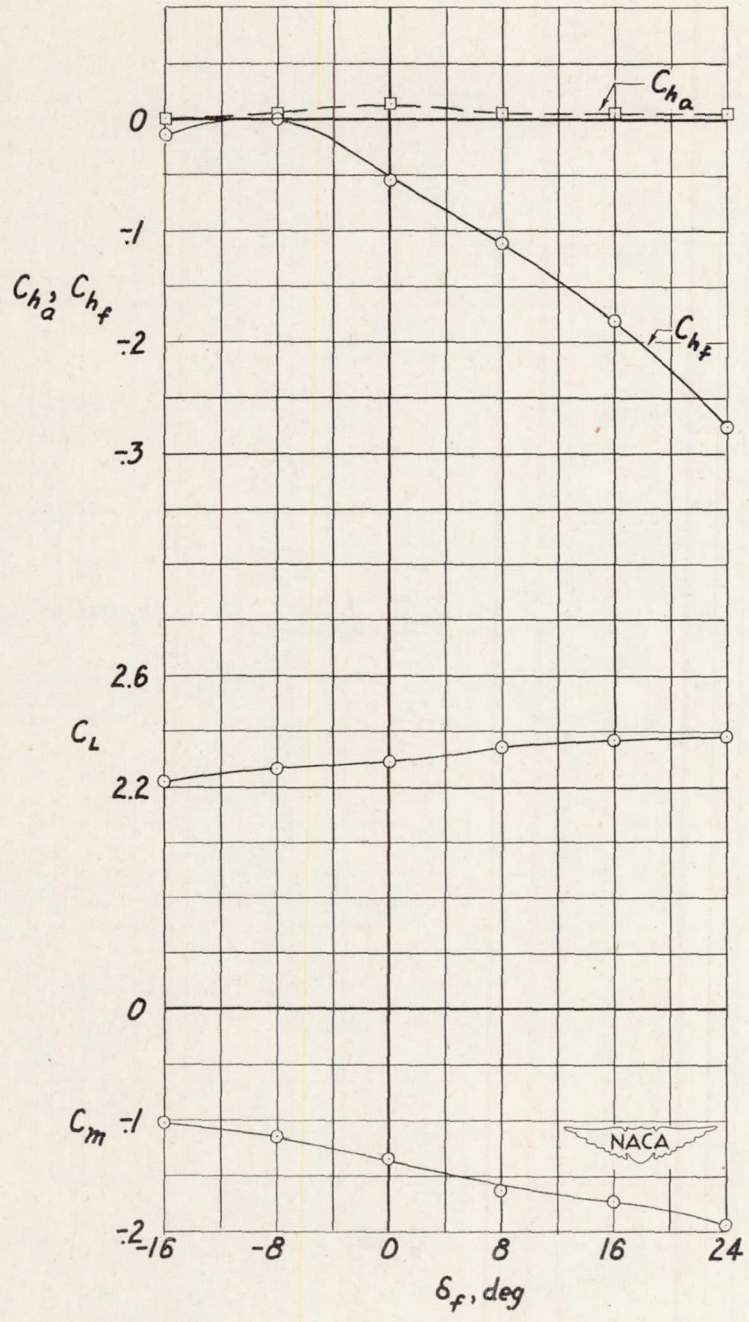

(a) $\alpha \approx 41^\circ$; $\frac{V}{nD} = 0.40$.

Figure 22.– Variation of C_m, C_L, C_{h_f}, and C_{h_a} with δ_f for conditions of $C_{D_R} = 0$. Articulated propellers; $\beta = 11.5^\circ$; $\delta_a = -48^\circ$.

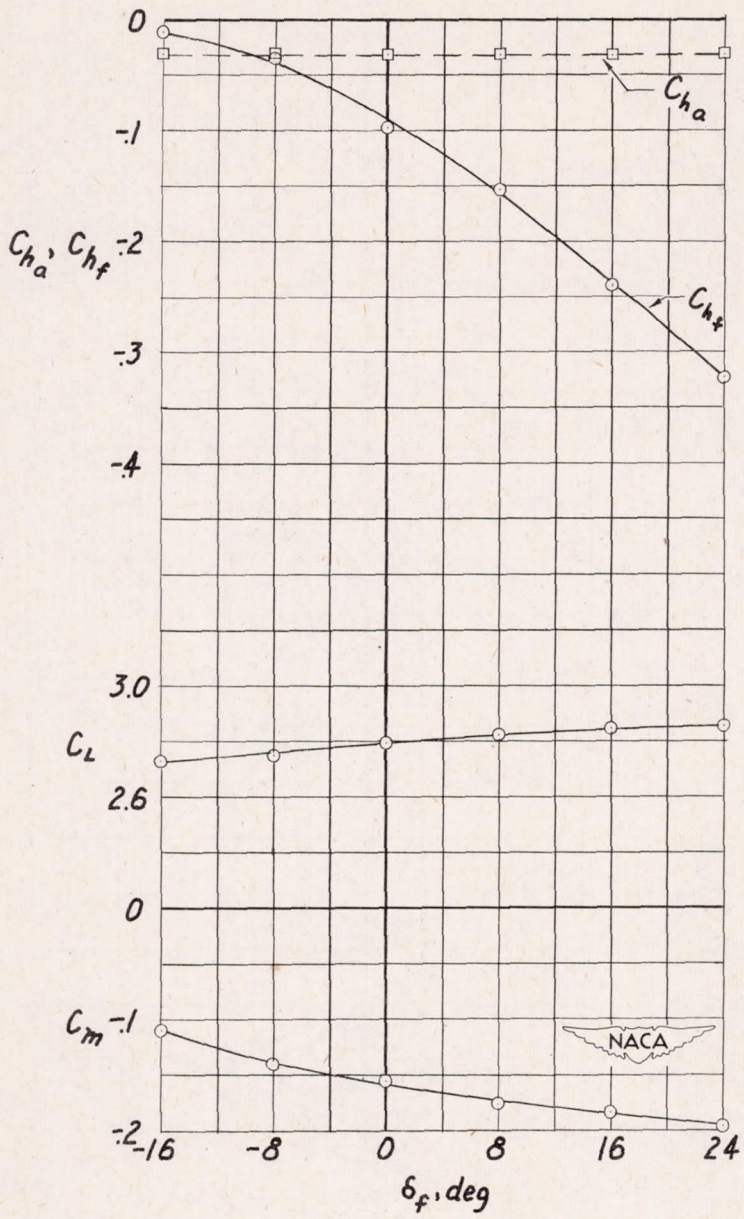

(b) $\alpha \approx 46^\circ$; $\frac{V}{nD} = 0.37$.

Figure 22.– Continued.

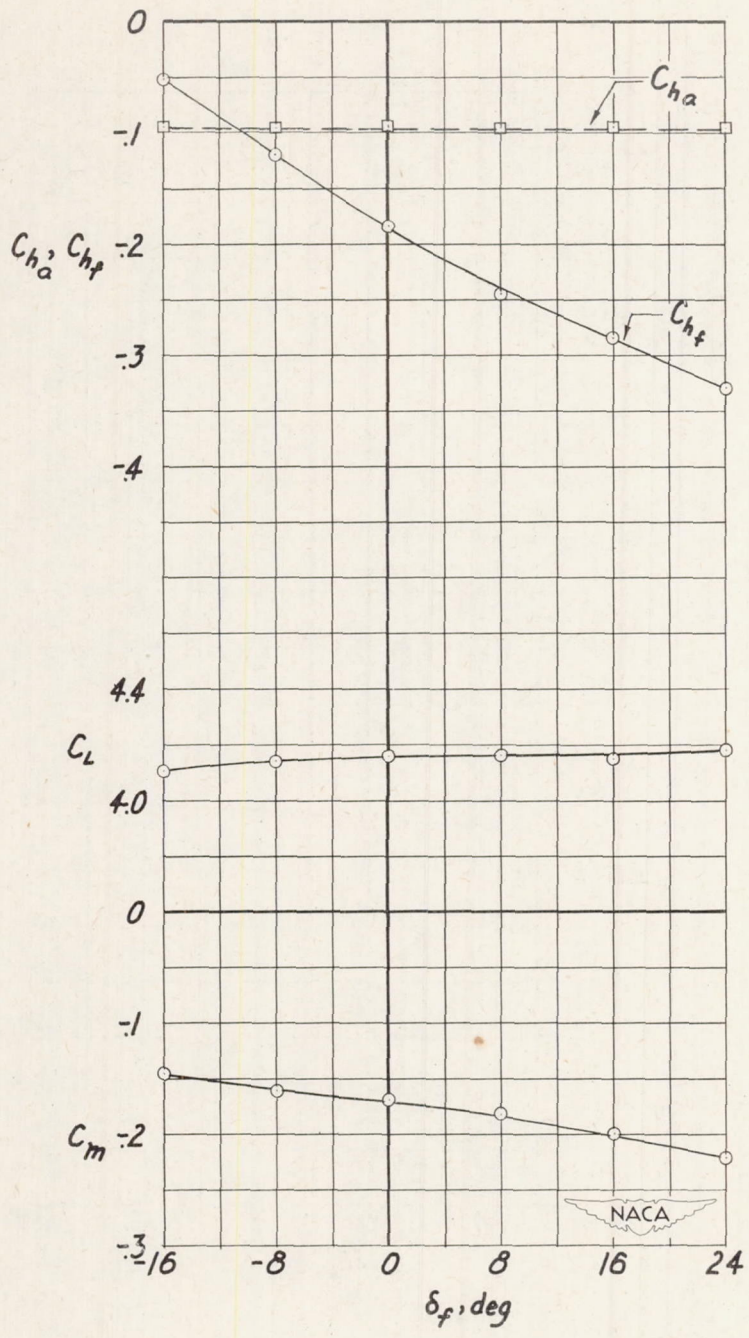

(c) $\alpha \approx 58°$; $\frac{V}{nD} = 0.30$.

Figure 22.– Continued.

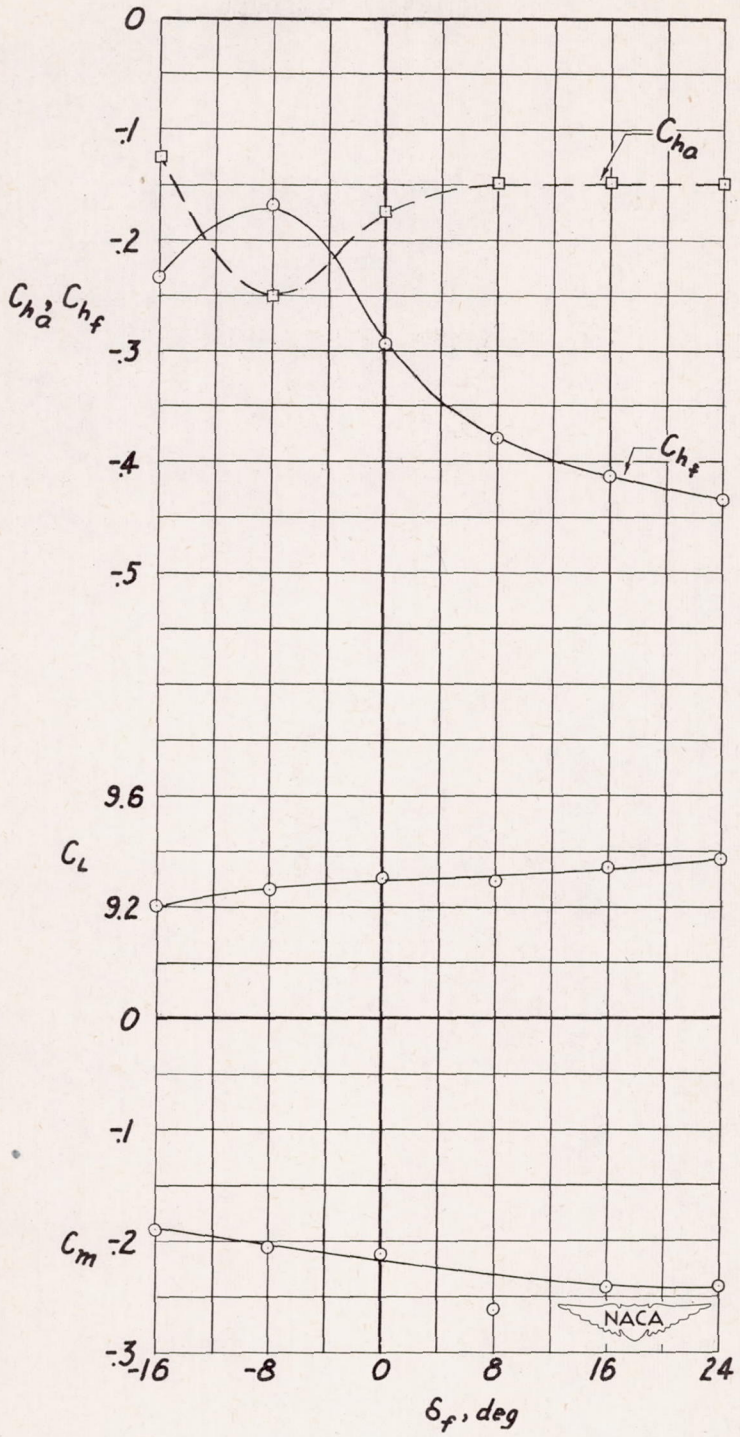

(d) $\alpha \approx 69°$; $\frac{V}{nD} = 0.20$.

Figure 22.– Concluded.